



Norwegian
Meteorological Institute
met.no

met.no report

no. 17/2010
SAR/HAZMAT/Leeway

Field Determination of the Leeway of Drifting Objects

The Leeway of a 20-ft Container, WWII Mine, Skiff, Sunfish, and a PIW in The Deceased Position

Fedje and Andfjord, Norway, September 2009

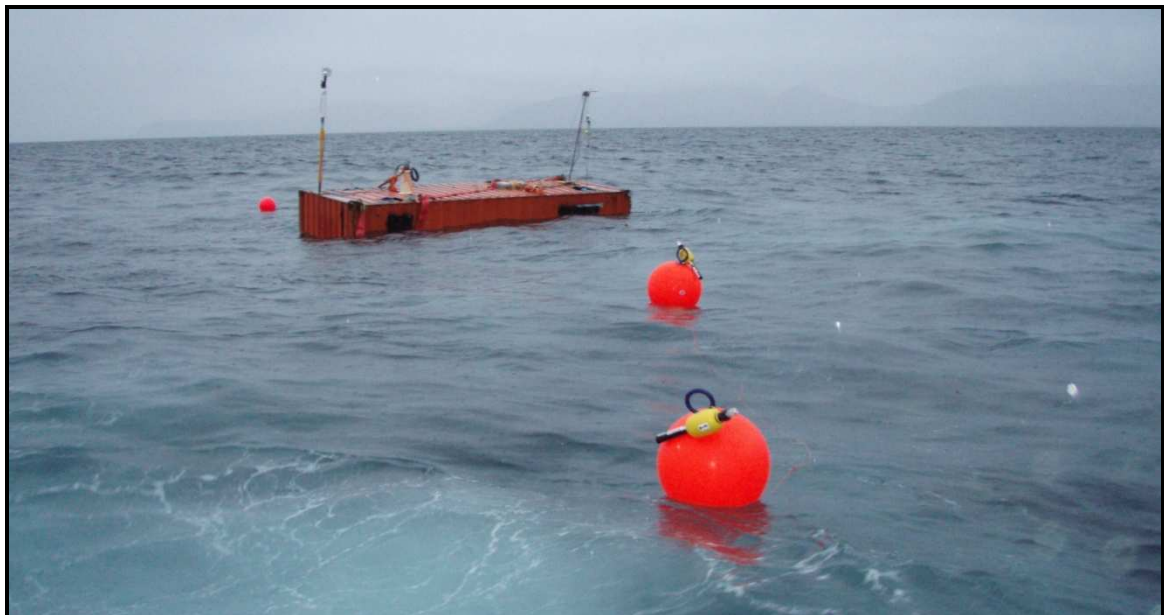
Arthur Allen (US Coast Guard)

Jens-Christian Roth (Royal Norwegian Navy)

Christophe Maisondieu (IFREMER)

Øyvind Breivik (The Norwegian Meteorological Institute)

Bertrand Forest (IFREMER)



Title Field Determination of the Leeway of Drifting Objects	Date 2010-08-27
Section VV	Report no. 17
Author(s) Arthur Allen, Jens Christian Roth, Christophe Maisondieu, Øyvind Breivik and Bertrand Forest	Classification <input checked="" type="checkbox"/> Free <input type="checkbox"/> Restricted
	ISSN 1553-8025
Client(s) NFR/FFN/Eureka	e-ISSN
	Client reference Eureka E!3652 SAR-drift
Abstract The leeway (windage) of five typical SAR/HAZMAT objects (person in water, mine, small sailboat, small open boat and a 20-ft container) and is studied. The method is applicable to objects smaller than 30m	
Keywords SAR, HAZMAT, trajectory models, leeway, windage, surface drift, operational oceanography	

Disiplinary signature	Responsible signature
_____	_____

Introduction

Search and Rescue (SAR), and hazardous material (HAZMAT) operational models include modules for the prediction of the drift of common SAR objects (Breivik and Allen, 2008) and HAZMAT materials and objects (Hackett *et al*, 2006; Davidson *et al*, 2009), and modules for planning the appropriate resource response. These models require algorithms of the wind and wave component of drift of the objects of interest. A review of the SAR and HAZMAT objects that has been studied by field experimentation before 1999 is presented by Allen and Plourde (1999). They made recommendation for 63 categories of objects to be included in SAR planning tools. Allen and Plourde provided the parameters for leeway speed as function of wind speed and a leeway divergence angle for all 63-leeway categories. Further work by Allen (2005) provided equations in the downwind and crosswind frame of reference for these same 63 categories. The predominance of operational SAR planning tools now uses either the equations from Allen and Plourde (1999) or Allen (2005). Allen and Plourde used an operational definition of leeway defined as:

□ Leeway is the velocity vector of the SAR object relative to the downwind direction at the search object as it moves relative to the surface current as measured between 0.3m and 1.0m depth caused by winds (adjusted to a reference height of 10m) and waves. □

This definition standardizes the reference levels for the measurements of leeway for SAR drift objects. Estimates of the velocity fields at both of these levels are readily available to the operational SAR planner.

Allen and Plourde (1999) organized the previous studied leeway objects into a hierarchical taxonomy based upon their leeway characteristics. This allowed the operator to select a class of object that best matches the search object for that particular case. They also clarified what objects have been studied, and by inference which objects have not been studied. It is the purpose of this particular work to conduct leeway field drift studies and add three additional objects to the existing list.

During this experimental field study, direct leeway measurements were made on a 4.15 meter open skiff, a Sunfish sailboat, a 20-foot full sized shipping container, and a person in water (PIW) in the deceased position. Continuing the efforts started in 2008 (Breivik *et al*, 2010), additional leeway data was collected on a World War II (WWII) L-Mk2, anchored mine. This report summarizes the results from this field study from a cruise off the coast of Fedje, Norway and second cruise in the Andfjord. An indication of the location of the two field areas is seen in Fig 1, while detailed close-ups of the areas are found in Figs 21, 30 and 39.

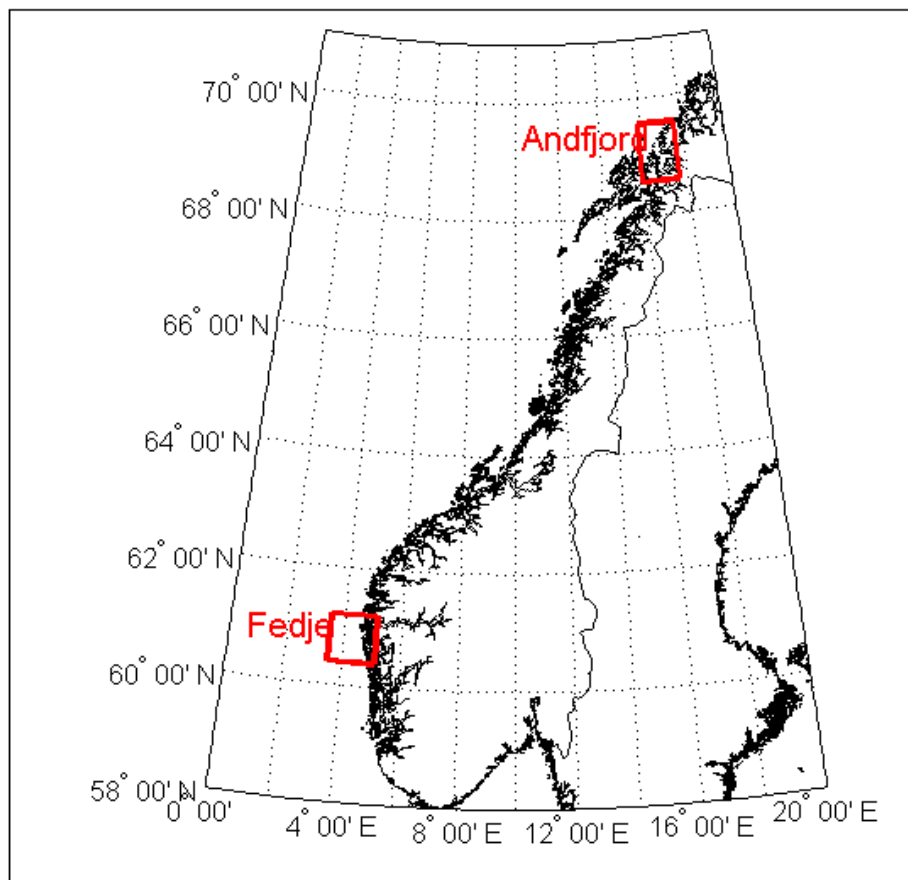


Figure 1. Coast of Norway, showing the experiment areas off Fedje and in the Andfjord.

Preparation of the Drifting Objects

The L-Mk2, anchored mine

The extensive use of sub surface, moored sea mines during WWII still poses a great threat to modern commercial shipping. Even though mine hunting operations were, and are still being carried out, old mine fields are still being detected. Occasionally the old moorings break and the mine rises to the surface and float under influence of wind and currents, posing a potentially lethal threat to whoever finds them. Knowledge on leeway behavior for mines is therefore important in order to track and predict where this ordnance drifts, before it can be safely dealt with by explosives experts.

A □dummy□ version of a moored L-Mk2 mine, Figs 2 and 3, was used during the experiment in order to properly study the leeway behavior of mines. The mine used in this experiments had an oval shape and measured 125 cm in length and had a 105 cm radius. The total weight was around 300 kg including 100 kg of sand in replacement for explosives. Roughly $\frac{3}{4}$ of the mine was submerged when it floats freely in the water.

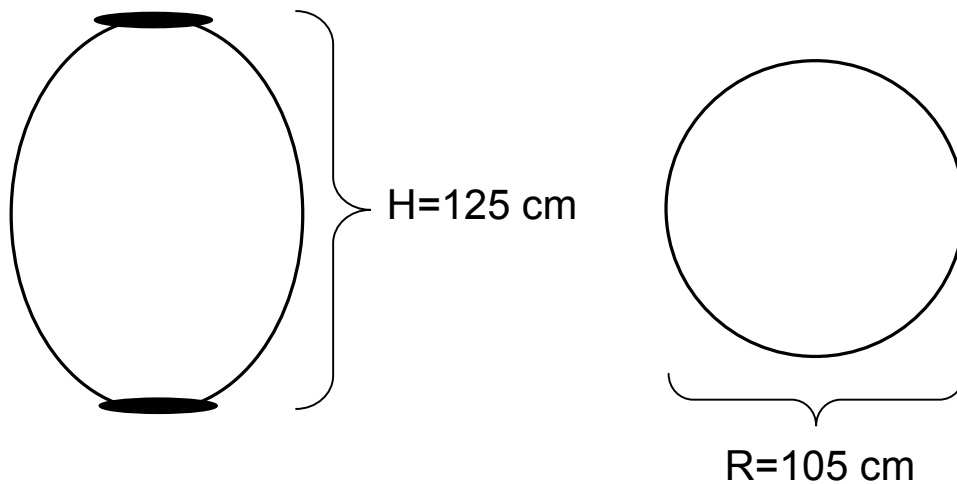


Figure 2: The mine measured 125 cm in length and had a radius of 105 cm. It contained 100 kg of sand in replacement for explosives and had a total weight of 300 kg.

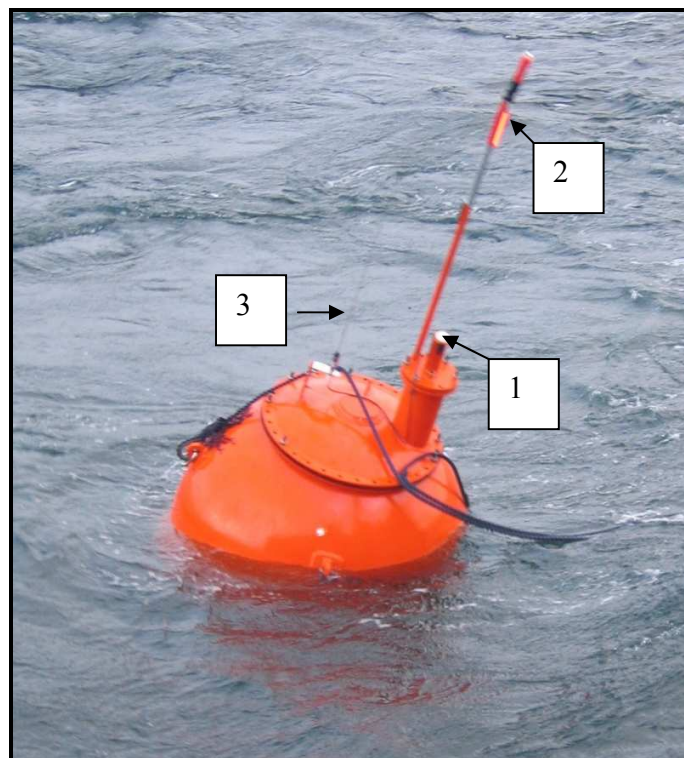


Figure 3: Roughly 3/4 of the mine was submerged when it floated freely in the water. Attached to the lid are a signal light (1), GPS antenna (2) and VHF antenna (3). The AIS unit was placed inside the mine.

The Skiff

A common SAR drift object is the open skiff or boat. A 4.15 m open skiff was studied during the Fedje cruise, Figs 4-6.

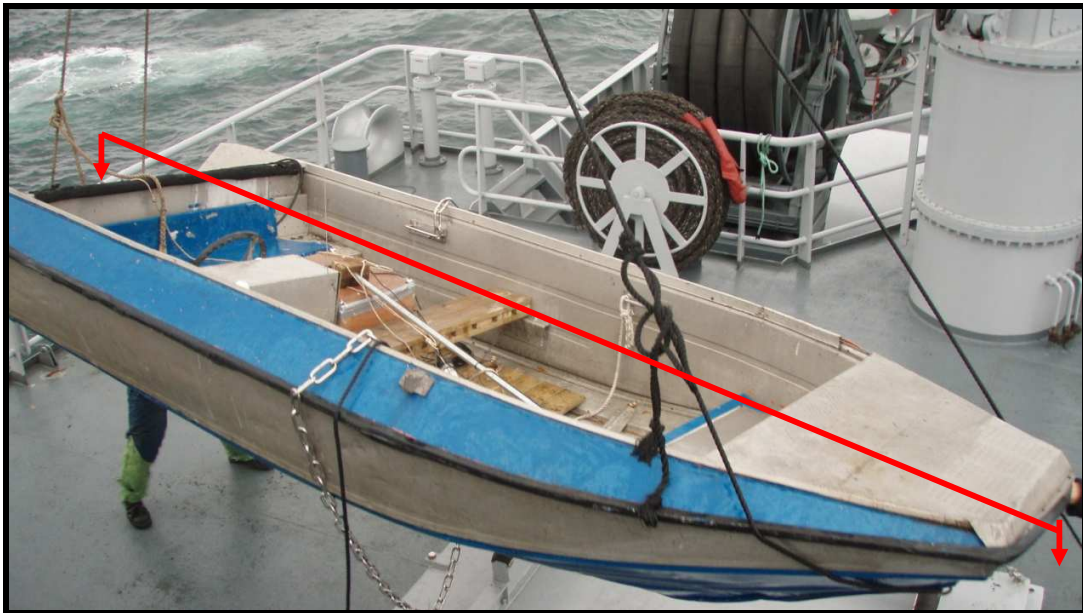


Figure 4. The 4.15 meter open skiff being recovered.

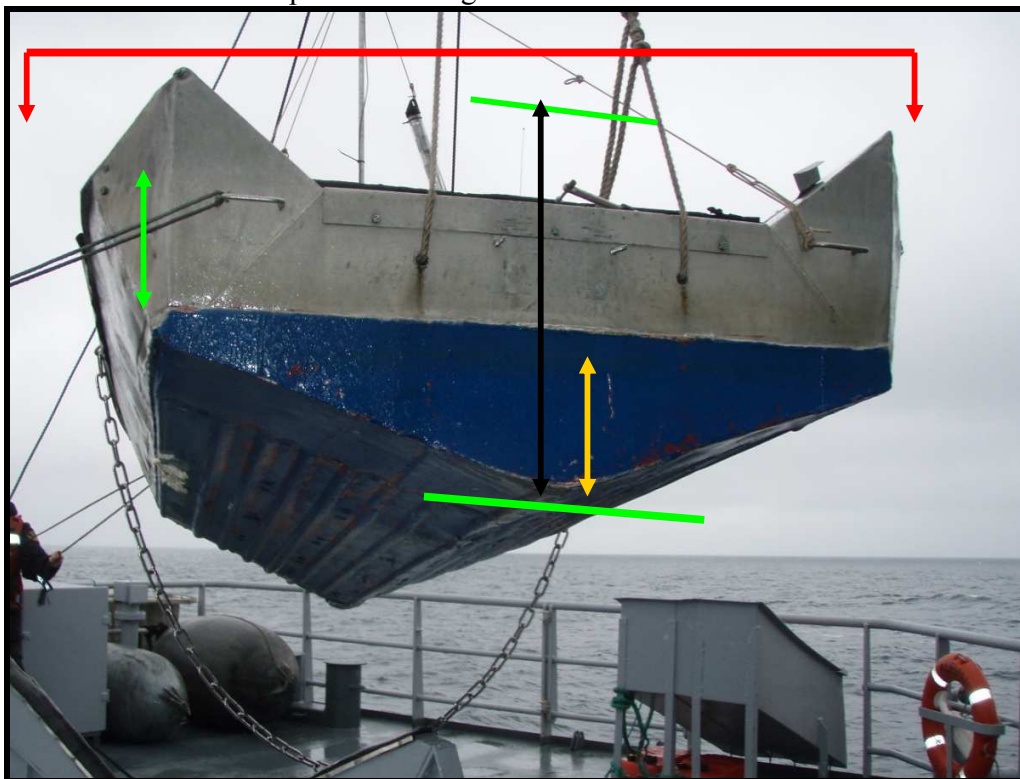


Figure 5. The stern of the 4.15 meter long boat, the beam is 1.70 meters (Red arrow), bottom to top distance is 0.82m (black arrow), rise is 0.27m (yellow arrow to top of blue

paint) and maximum beam was 0.38 cm (green arrow) from top of the blue paint. Also shown is the chain that hung below the center point of the skiff to which was attached to the 10m floating line of the S4 EMCM suspended beneath a red fishing float.



Figure 6. The 4.15 meter open skiff deployed. Sonic anemometer at 2.0 meters above water line, yellow Novateck combo flasher VHF beacon on board, and the red fishing float above the S4 EMCM are all visible.

The Sunfish Sailboat

The Sunfish sailboat is a one-man, beach-launched sailing dingy utilizing a pontoon type hull carrying a lateen sail mounted to an un-stayed mast (see Fig 7). The Sunfish was first manufactured in 1952 and as of 2001 over 300,000 have been sold. This makes the Sunfish the most common single-designed sailboat in the world. The hull is fiberglass, foam-filled and enclosed. The small cockpit has self-drainer. The rudder is designed to kick-up upon beaching the sailboat. For this experiment, the Sunfish was configured without sail and rudder. A plywood dagger board (false keel) was fitted, but tended to fall off. Hence, the leeway estimates are based on drifts with and without the dagger board. The mast was exchanged for a Coastal Environmental Systems WeatherPak wind monitoring system was mounted to provide wind measurements for this drift object and nearby test drift objects (see Figs 8 and 9). The deck and hull just aft of the Sunfish mast mounting hole was cut open to prepare a mount for the ADCP's gimbal and head. The ADCP was mounted so the bottom of the head was flush with the bottom of the Sunfish's hull. The WeatherPak mast's bottom bracket was bolted just forward of the ADCP and aft of the Sunfish's mast mounting hole. To simulate weight of person on board, the AIS, ADCP battery and WeatherPak battery canisters were mounted in the well where persons on board the Sunfish would normally place their feet. In emergency situations this would be the location of survivors.

- **LOA:** 4.2 m (13'9")
- **Beam:** 1.24 m (4'1")

- **Draft:** 0.89 m (2'11")
- **Sail Area:** 6.97 m² (75 square feet)
- **Hull Weight:** 54.4 kg (120 lb)
- **Capacity:** 1-2 people

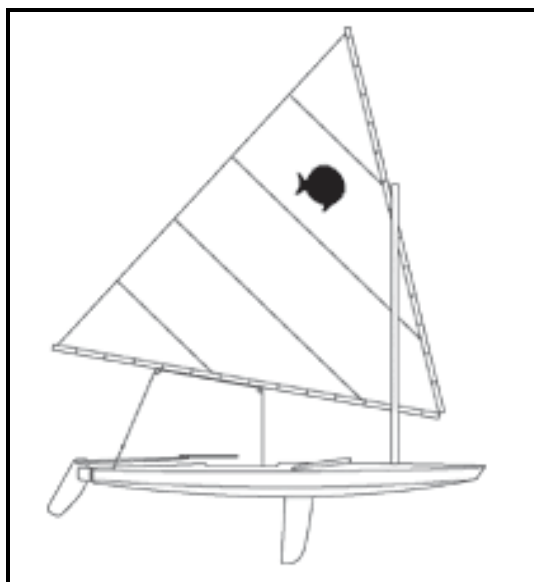


Figure 7. Sunfish sailboat. (Sailing configuration)



Postal address
P.O.Box 43, Blindern
NO-0313 OSLO
Norway

Office
Niels Henrik Abelsvei 40

Telephone
+47 22 96 30 00

Telefax
+47 22 96 30 50

e-mail: met@met.no
Internet: met.no

Bank account
7694 05 00628

Swift code
DNBA20KK

Figure 8. Sunfish, configured for leeway drift study. Arrows point to: (1) AIS, (2) ADCP battery, (3) WeatherPak battery canister (4) gimbal for ADCP head, (5) RDF/ flasher beacon, (6) R.M. Young anemometer, and (7) WeatherPak.



Figure 9. Sunfish deployed.

Person-in -Water (PIW) in the deceased position

A man-overboard manikin was modified to be a PIW in the deceased position. The head of the manikin was an Aanderaa spherical 8kg buoy that contained a GPS receiver and AIS beacon. This allowed us to track and recover the manikin. A Nortek AquaDopp 1 MHz ADCP was tied to the legs at the crotch of the manikin, pointing downward. The AquaDopp is 55cm cylinder with 7.5 cm diameter, Fig 10. The top (battery end) was tied so there was some freedom to hang downward from the legs. The AIS buoy was free to swing around so that its antenna was upright when the manikin was deployed.



Figure 10. PIW manikin rigged for deployment, lying face up. An AIS-transmitting buoy is mounted as its "head" while an AquaDopp current meter is mounted from its waist.



Figure 11. Manikin deployed as a PIW in the deceased position.

20-ft Container

The nominal exterior dimensions of the 20-foot standard shipping container is 19.875 feet (6.058 m) long by 8.0 feet (2.438 m) wide by 8.5 feet (2.591m) high which can hold internally 1170 cubic feet or 33.131 cubic meters. The 20-ft container was equipped with an AIS beacon, the sonic anemometer, and a S4 EMCM and upward looking Nortek AquaDopp acoustic doppler current profiler (ADCP), see Fig 12. The two current meters were attached to tag line along with a Novatech combo Flasher/RDF beacon. During the second deployment, a Coastal Environmental Systems WeatherPak wind monitoring system was added.

Postal address
P.O.Box 43, Blindern
NO-0313 OSLO
Norway

Office
Niels Henrik Abelsvei 40

Telephone
+47 22 96 30 00

Telefax
+47 22 96 30 50

e-mail: met@met.no
Internet: met.no

Bank account
7694 05 00628

Swift code
DNBANOKK



Figure 12. The 20-ft container deployed. The WeatherPak meteorological mast is on the left and the sonic anemometer on the right. The two orange fishing floats with flashers and RDF beacons support the EMCM and ADCP current meters.

Barrels inside the container provided flotation (see Fig 13). Holes were cut in the bottom and sides of the container to allow the container to fill and drain during deployment and recovery. During both drift runs the freeboard of the container was 50 +/- 5 cm. Therefore the percent immersion was $(2.591\text{m}-0.50\text{m})/2.591\text{m}$ or 80.7% +/- 2.0%.

Postal address
P.O.Box 43, Blindern
NO-0313 OSLO
Norway

Office
Niels Henrik Abelsvei 40

Telephone
+47 22 96 30 00

Telefax
+47 22 96 30 50

e-mail: met@met.no
Internet: met.no

Bank account
7694 05 00628

Swift code
DNBANOKK



Figure 13. Interior of container, showing some of the plastic barrels hung from the ceiling of the container to provide buoyancy. The sling in the middle of the ceiling provides a hold for the sonic anemometer electronics and batteries as well as the AIS beacon.

Instrumentation

Each drift object was equipped with gear for deployment, drift and recovery as well as data collection. The drift objects were ballasted and augmented with extra floatation to mimic the un-equipped distress configuration as closely as possible. The skiff, Sunfish, and container all required lifting bridles for deployment and recovery. Very High Frequency (VHF) strobe-flashers, and Automatic Identification System (AIS) beacons were used to aid in the tracking and recovery of these three drift objects, while the PIW was tracked only by AIS. The AIS contained a GPS data logger which provided the over the-ground displacement data.

During this experiment, AIS Class-B transponders were used to track the drift objects via GPS and to provide a means to locate and recovery them. The AIS consists of a VHF transponder and receiver which is connected to a GPS, broadcasting a signal every 2 to 10 seconds while underway. For the experiment, three Class-BIS transponders were built as self contained units consisting of an AIS unit, a 24 Ah battery, a GPS antenna, a VHF antenna and a data logger, all fitted into a watertight pelican case, see Fig 14.

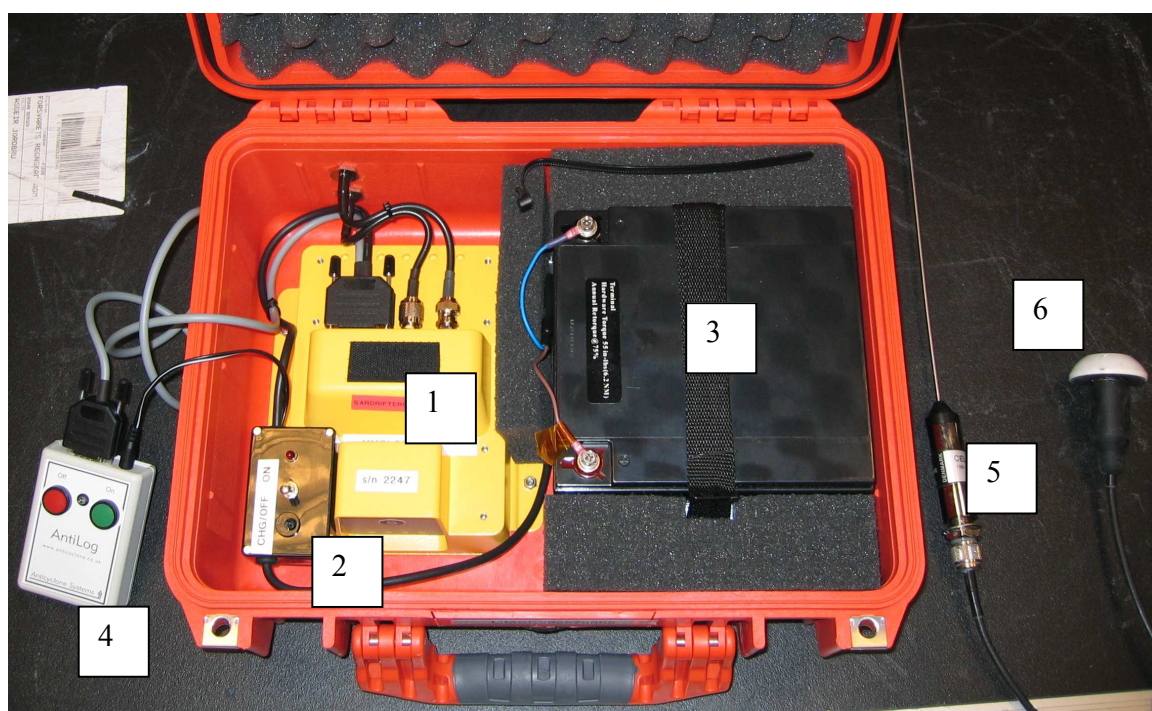


Figure 14. The AIS unit consist of an AIS transponder (1), on/off switch (2), battery (3), data logger (4), VHF antenna (5) and a GPS antenna (6). All parts, except the two antennas, are fitted into the pelican case.

The 4.15-m open skiff and the 20-ft container had InterOcean S4 Electromagnetic current meters (EMCM) attached via a 30 meter line. The S4 current meter was suspended in an

aluminum frame at 75 cm depth, see Fig 15. A fishing float was attached to the top of the frame. The float was attached by 30 meters of line to the pull point on the skiff or container. The S4 EMCM sampled at 2 Hz, and the samples were internally averaged over 1200 samples or 10 minutes. Sampling periods were started on the 10:00 minutes. The samples were rotated $\pm 1.03^\circ$ (Fedje) and -5.39° (Andfjord) from magnetic north to true (geographical) north. The values were then rotated 180 degrees to account for the current meters being pulled through the ambient water by the drift object. The records were then trimmed at both ends to eliminate any effects of deployment and recovery. This often required that the initial full ten-minute sample in the water after deployment was discharged, as during this period the drift object is still adjusting to its equilibrium orientation with the wind, and is perhaps still affected by the vessel's bow thrusters.



Figure 15. S4 EMCM in an aluminum frame. The top of the frame is toward the bottom of this picture, where a fishing float would be attached. The 30-meter line would be attached to the bracket at the long end of the frame.

The Sunfish contained a downward looking RD Instrument Workhorse Monitor 1228.8 kHz ADCP, see Fig 16. The RDI ADCP was programmed to 10 bins of 5 cm bin size, blanking range of 25 cm, binning at 1.0 Hz, and averaging over 1:00 minutes. Data was then averaged over the top 9 bins and 10-minute intervals on the 10 minutes. Averages were rotated for magnetic ($\pm 1.03^\circ$ or -5.39°) and leeway (180°) coordinates systems, equivalent to the S4 current meter data. The first bin was 42 cm below head and the last bin was 92 cm below. The head was 25 cm below waterline, so data was collected between 67 cm and 117 cm depth. The 10-minute samples were then trimmed at both ends to eliminate any effects of deployment and recovery.



Figure 16. The downward RD Instrument Workhorse Monitor 1228.8 kHz Acoustic Doppler Current Profiler (ADCP) mounted in a gimbal in the Sunfish. The bow of the Sunfish is to the right. Extra flotation can be seen around the current meter.

The PIW had a downward-looking Nortek AquaDopp 1MHz ADCP tied to the waist, see Fig 10. For Run 1 of the PIW, the AquaDopp was programmed to 10 bins of 25 cm bin size, blanking range of 20 cm, with a transmit distance of 27 cm, sampling at 1.0 Hz, and averaging over 1 minute. The average depth of the sensor head was 34 cm, hence the first sample bin was centered at 80 cm depth and the second at 106 cm. Data was then averaged over the top 2 bins. For Run 3, the AquaDopp was programmed with 10 bins of 50 cm size, blanking range of 40 cm and a transmit distance of 55 cm. The average depth of the sensor head was 23cm. Therefore, for Run 3, we used only the first sample cell centered on 115cm depth. One-minute averages were rotated for magnetic (-5.39°) and leeway (180°) coordinate systems and then averaged to 10-minute samples. The 10-minute samples were finally trimmed at both ends to eliminate any effects of deployment and recovery.

The 20-ft container had an upward-looking Nortek AquaDopp 1MHz ADCP suspended from a second float attached to the far end of the S4 EMCM frame. For the container runs, the Nortek AquaDopp was programmed to 10 bins of 50 cm bin-size, blanking range of 40 cm, with a transmit distance of 55 cm and a sampling rate of 1.0 Hz. Runs 1 and 2 were averaged over 10 minutes. The average depth of the sensor head was 415 cm, hence the sixth sample bin was centered at 60 cm depth and fifth at 112 cm. Data were then averaged over these two top bins. One-minute or ten-minute averages were rotated for magnetic (-5.39°) and leeway (180°) coordinates systems and then 1-minute samples were averaged to 10-minute samples. The 10-minute samples were then trimmed at both ends to eliminate any affects of deployment and recovery.

The Coastal Environmental System WeatherPak 2000 with R.M. Young anemometer collected the winds aboard the Sunfish and the 20-ft container during its Run 2. The height of the R.M Young on the Sunfish was 235 cm above water line. The R.M Young was 200 cm above the top of the container, and the container top was 50 cm above the waterline. The anemometers was sampled at 1 Hz and averaged over 10-minute samples on the 10:00. GPS positions were collected by the AIS system on board the container. The positions closest to the 10:00 were used to determine the over the ground drift rate of the container. These values were then used to convert from relative winds to absolute winds at the height of the anemometer. Wind speeds were adjusted under neutral conditions to a height of 10-meters, following Smith (1988).

The sonic anemometer CV7, manufactured by LCJ Capteurs, collected winds aboard the 4.15m skiff at 2.0 meters above sea level and aboard the 20-foot full-sized shipping container at 2.50 meters above sea level, see Figs 6 and 12. This sensor was chosen because it is light and rugged. The CV7 has a very low threshold of 0.1 m/s wind speed, with a resolution of 0.05 m/s, and a range from 0.1 to 40 m/s. Directional sensibility is $\pm 1^\circ$ and resolution is 1° . The direction provided by the anemometer is the direction relative to the main axis of the transducer. In order to obtain the absolute wind direction, the anemometer must be coupled with a compass and positioned in a referenced frame. The referential chosen here was the main longitudinal axis of the skiff or the container. The absolute wind direction was then to be obtained from the compass (3D earth magnetic field data) of the motion record unit placed on-board the container. This compass has a 0.1° alignment error and a linearity of 0.2% of full scale. Unfortunately, control calibration tests carried out after the trials showed that the compass was not providing stable results because of a failure of the magnetic field sensors. Therefore wind directions were taken from the WeatherPak systems.

Afterwards, records were matched in time for analysis on the 10-minute samples. The leeway was decomposed into downwind and crosswind components for every 10-minute sample. The winds from the Sunfish were used for the L-MK2 mine, the 4.15m skiff, the PIW in the deceased position, and the Sunfish itself. The leeway speed and the downwind components were linearly regressed against the 10-m wind speed. The linear regression was done both unconstrained and constrained through the origin. The slope, y -intercept (for the unconstrained regression), Standard Error term ($S_{y,x}$) and the r^2 term were estimated following Neter et al. (1996). For the crosswind components of leeway, the values were separated along runs or portions of runs which were found by the progressive vector diagrams (PVD) to be consistently left (negative) or right (positive) of the downwind direction. Finally all left and right-drifting crosswind estimates were combined and linearly regressed against the 10-m wind speed, again both unconstrained and constrained through the origin.

The Field Experiments

Four drift runs were conducted in the period 10-14 September 2009 off Fedje, Norway by the Norwegian Coast Guard vessel (Kystvakten) CGV Ålesund. The drift objects during

this cruise were the Sunfish, the WWII mine, and the 4.15m open skiff. Table 1 is a summary of the individual drift runs for this first cruise.

Three drift runs were conducted in Andfjord in the period 24-27 September 2009 by CGV Harstad. The drift objects were the Sunfish, a full-sized 20-foot shipping container, a Person-in-the-Water manikin in the deceased position. Furthermore, the drift of a small buoy equipped with an AIS transmitter was subjectively compared with that of the PIW, but no leeway estimates were made. Table 2 is a summary of the individual drift runs for this second cruise. The two experiment areas are shown in Fig 1, while close-ups are shown in Figs 21, 30 and 39.

Table 1. Summary of Leeway 2009 Drift Runs Fedje 10-14 September 2009

Object	Run	Start time DD/hh:mm(z)	End Time DD/h:mm(z)	Current meter	Wind Source	Position
Sunfish	1	10 / 21:00	11 / 07:40	RDI ADCP	WPak885	AIS
Mine	3	10 / 21:20	11 / 07:30	S4 EMCM	Sunfish	AIS
Skiff	1	10 / 21:20	11 / 06:20	S4 failed	Sonic	AIS
Sunfish	2	11 / 10:50	12 / 07:00	RDI ADCP	Wpak 885 (failed)	AIS
Mine	4	11 / 10:50	11 / 15:20	S4 EMCM	Sonic	AIS
Skiff	2	11 / 11:00	11 / 14:30	S4 failed	Sonic	AIS
Skiff	3	11 / 17:10	12 / 08:30	S4 failed	Sonic	AIS
Sunfish	3	12 / 20:20	13 / 11:20	RDI ADCP	WPak884	AIS
Mine	5	12 / 20:40	13 / 11:20	S4 EMCM	Sunfish	AIS
Skiff	4	12 / 20:40	13 / 10:20	S4 EMCM ADopp failed	Sunfish Sonic	AIS
Sunfish	4	13 / 15:10	14 / 07:00	RDI ADCP	WPak884	AIS
Mine	6	13 / 15:20	14 / 06:50	S4 EMCM	Sunfish	AIS
Skiff w/ 4 sand bags	5	13 / 15:40	14 / 06:10	S4 EMCM	Sunfish	AIS

Black = Data processed through to 10-minute samples

Red = instrument failed, not available

Blue = record ends before [End Time]

Table 2. Andfjord, 24-27 September 2009

Object	Run	Start time Day / hh:mm(z)	End Time Day / hh:mm(z)	Current meter	Wind source	Positioning
Cont	1	24 / 09:10	25 / 05:20	S4 & Adopp (separated)	Sonic	AIS
Sunfish	5	24 / 09:40	25 / 09:10	RDI	Wpak 884	AIS
PIW	1	24 / 17:40	25 / 05:30	ADopp	evaluating	GPS
AIS	1	24 / 17:40	25 / 05:30	none	evaluating	GPS
Sunfish	6	25 / 17:50	25 / 20:00	RDI	Wpak 884	GPS
PIW	2	25 / 18:00	25 / 20:20	ADopp	Sunfish	GPS
MOB	2	25 / 18:00	25 / 20:20	none	Sunfish	GPS
Cont	2	27 / 05:40	27 / 16:40	Adopp & S4	Sonic & Wpak	GPS
PIW	3	27 / 05:40	27 / 14:40	ADopp	Cont	GPS
MOB	3	27 / 05:40	27 / 16:40	none	Cont	GPS

Empirical Leeway Estimates

The leeway of the drifting objects was empirically estimated from the current meter measurements in conjunction with the wind speed and direction estimates following Allen (2005) and Breivik and Allen (2008).

The Leeway of the WWII L-MK2 Mine

Four separate drift runs were conducted on three drift objects during an earlier experiment from 31 March to 3 April 2008 by CGV Ålesund off Fedje, Norway. The results from that experiment were reported by Breivik *et al* (2010). Leeway data were successfully collected from one drift run for the WWII mine during the 2008 field experiment. The data from that run was added to WWII mine drift runs from the September 2009 Fedje experiment. The drift runs of the World War II L-Mk2 Mine that successfully returned concurrent leeway and wind data are summarized in Table 3.

The leeway speed and the downwind component of leeway versus the 10-m wind speed for the mine are shown in Figs 17 and 18, along with the unconstrained and constrained linear regressions and their respective 95% prediction limits. Tables 7 and 8 summaries the linear regression slope, y -intercept terms, r^2 and standard error (S_{yx}) terms for the leeway speed and the downwind component of leeway.

Table 3. Summary of WWII L-MK2 Mine Leeway Drift Runs

Drift Object Run	Start		End		Duration		10 m Wind Speed Range
	Time	Date	Time	Date	Hr	Min	m/s
	UTC		UTC				
Run 2	15:10	1 April 2008	06:00	2 April 2008	14	50	0.2 □ 10.4
Run 3	21:20	10 Sept. 2009	07:30	11 Sept. 2009	10	10	3.7 □ 6.1
Run 4*	11:00	11 Sept. 2009	14:30	11 Sept. 2009	4	30	6.6 □ 9.3
Run 5	20:40	12 Sept. 2009	11:20	13 Sept. 2009	14	40	7.0 -10.5
Run 6	15:20	13 Sept. 2009	06:50	14 Sept. 2009	15	30	0.0 □ 11.9

* Drift Run 4 winds from the Sonic Anemometer board the skiff, which returned only wind speed. Therefore Drift Run 4 was available for only the leeway speed versus wind speed, since it could not be decomposed into Downwind and Crosswind components of leeway.

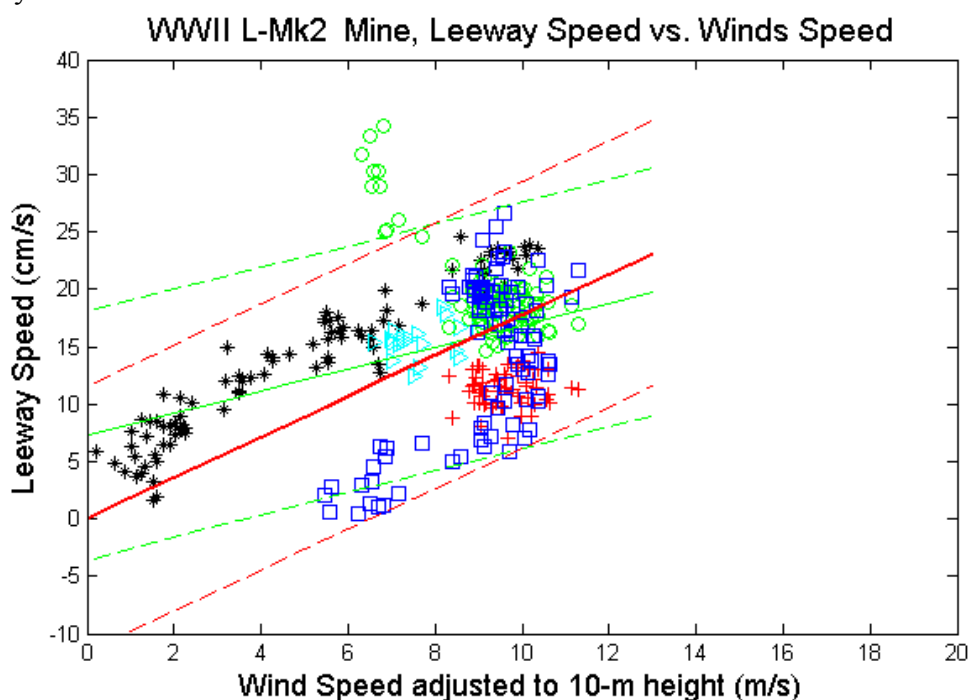


Figure 17. Leeway Speed (cm/s) versus Wind Speed adjusted to 10-meter height for the WWII L-MK2 mine. Unconstrained linear regression mean (solid) and 95% confidence levels (dash) are plotted in green. Constrained linear regression is plotted in red. Run 2 (back *), Run 3 (red +), Run 4 (cyanide ►) Run 5 (green o) Run 6 (blue □)

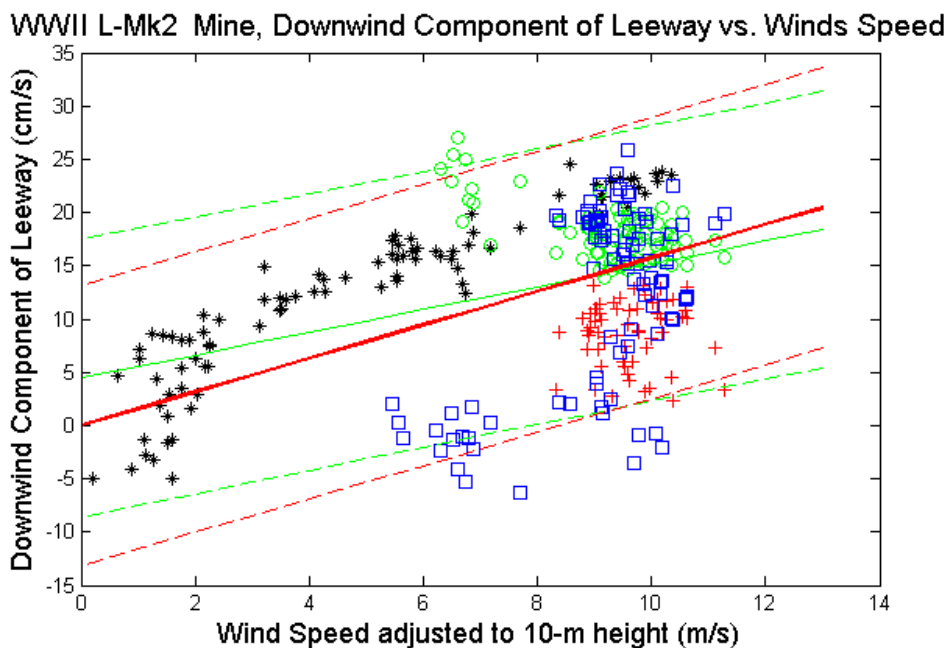


Figure 18. Downwind component of Leeway (cm/s) versus Wind Speed adjusted to 10-meter height for the WWII L-MK2 mine. Unconstrained linear regression mean (solid) and 95% confidence levels (dash) are plotted in green. Constrained linear regression is plotted in red. Run 2 (back *), Run 3 (red +), Run 5 (green o) Run 6 (blue □)

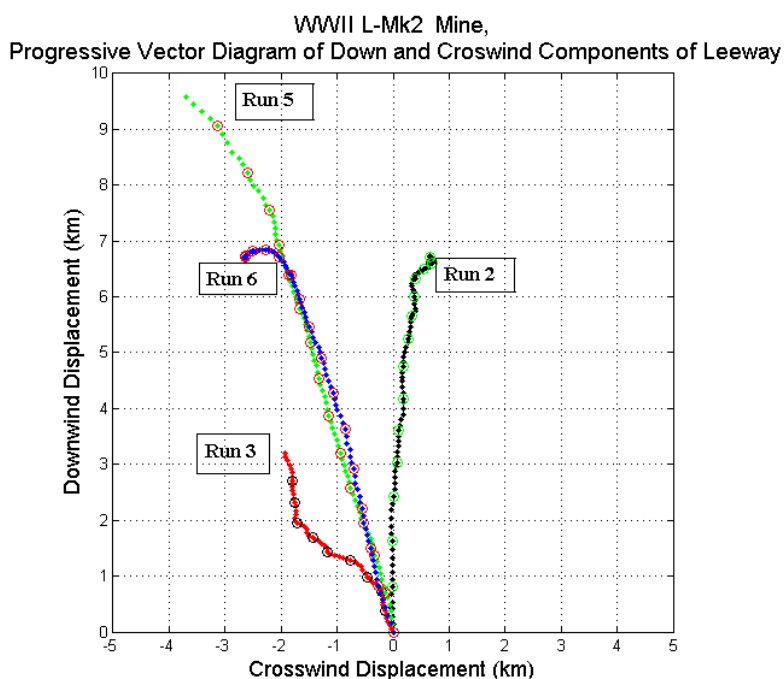


Figure 19. Progressive Vector Diagram (PVD) of the downwind and crosswind components of leeway displacement for the WWII L-MK2 mine. Downwind is up, and positive crosswind is to the right. Displacement is given in kilometers. Hourly intervals are indicated by a hatched point every 6th point.

The Crosswind components of leeway were separated into Positive Crosswind components (Run 2), and Negative Crosswind components (Runs 3, 5 and 6) as shown in Fig 19 of the Progressive Vector Diagram of the downwind and crosswind components. Since separation of the crosswind components of leeway results in two smaller data, the crosswind components were re-combined by adding the negative of the Negative Crosswind components to the Positive Crosswind Components and performing the regression of the combined data set against the 10-meter wind speed, as seen in Fig 20. With this limited data set we were unable to collect sufficient data characterize differences between the positive and negative components of crosswind leeway.

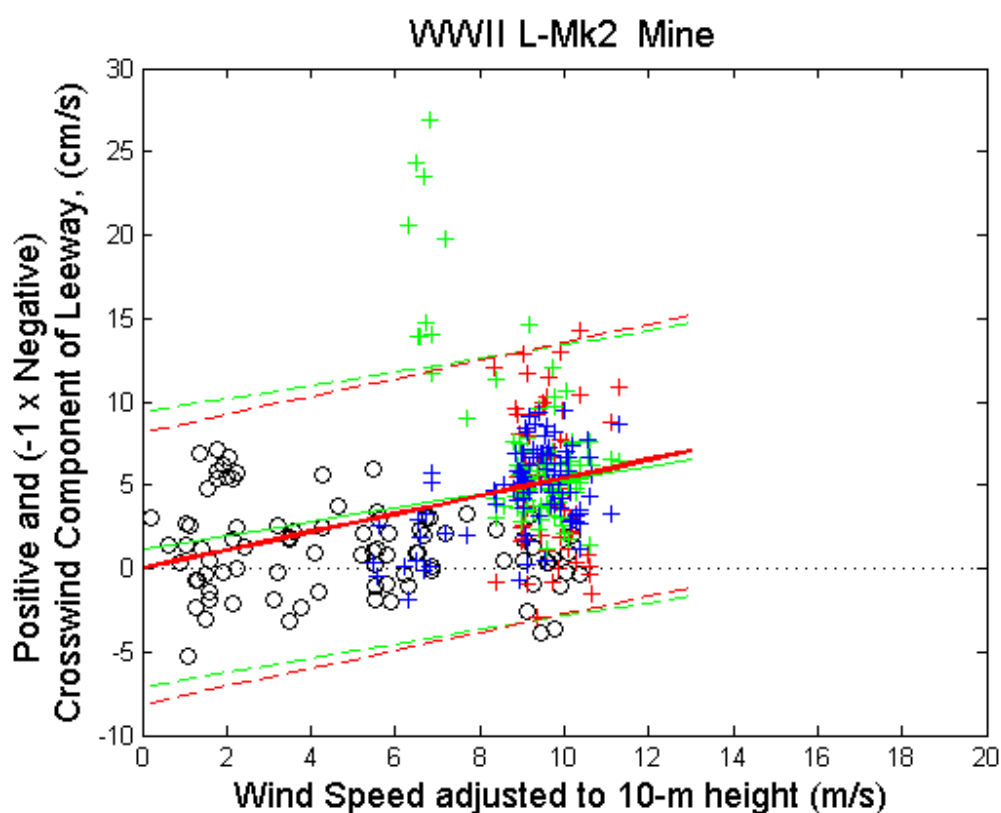


Figure 20. The combined estimate of the crosswind leeway component composed of positive (right-drifting) and negative (left-drifting) crosswind estimates (cm/s) versus 10-m wind speed for the WWII L-MK2 mine. Unconstrained linear regression (solid) and 95% confidence levels (dashed) are plotted in green. Constrained linear regression is plotted in red. Positive CWL values from Run 2 are plotted in black (o). Negative CWL values are Runs 3 (red +), Run 5 (green +) and Run 6 (blue +).

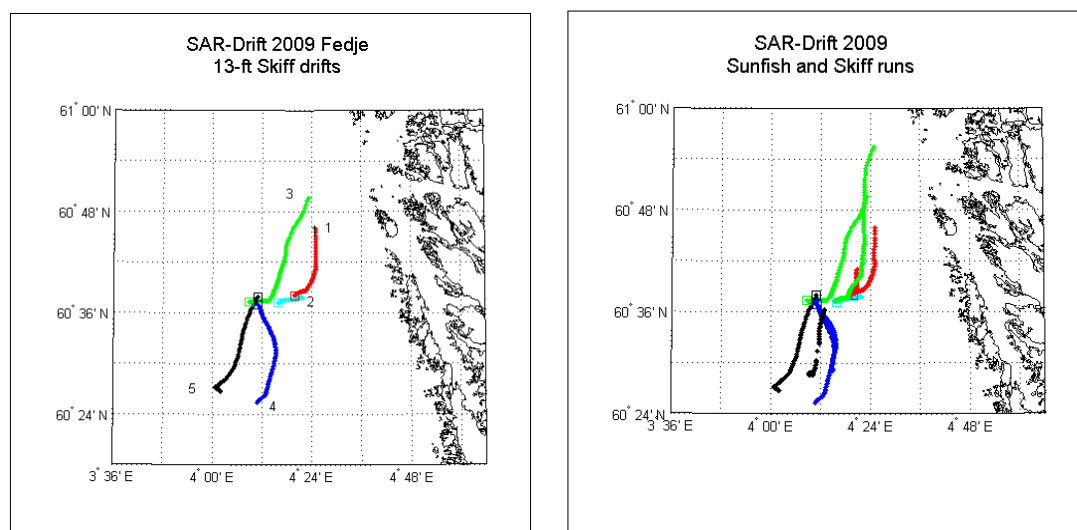
The Leeway of the Skiff

Leeway data was successfully collected from two drift runs for the 4.15 meter skiff during the September 2009 Fedje Leeway Drift experiment. The drift runs of the upright shallow-v hull 4.15m skiff that successfully returned concurrent leeway and wind data are summarized in Table 4. The skiff was empty during Run 4 while in Run 5 four sand bags weighing 30kg each were added to the skiff to simulate the weight of survivors.

Table 4. Summary of 4.15 meter (13.6 foot) open □upright, shallow-v hull skiff Leeway Drift Runs

Drift Object Run	Start		End		Duration		10 m Wind Speed Range
	Time	Date	Time	Date	Hr	Min	m/s
	UTC		UTC				
Run 4 (empty)	20:40	12 Sept. 2009	10:20	13 Sept. 2009	13	40	7.0 □10.5
Run 5 (4 sand bags)	15:30	13 Sept. 2009	02:40	14 Sept. 2009	11	10	0.1 □11.9

The leeway speed and the downwind component of leeway of the skiff versus the 10-m wind speed are shown in Figs 21 and 22 along with the unconstrained and constrained linear regressions and their respective 95% prediction limits. Fig 23 is the progressive vector diagram of the downwind and crosswind components of leeway displacement. We can see that Run 4 is primarily left of downwind direction and Run 5 is primarily to the right. Note that the crosswind component is horizontally exaggerated 2x the downwind displacement; with the data separated by the two runs, positive (right of downwind) and negative (left of downwind) components of leeway versus the 10-m wind speed. Also shown are the unconstrained and constrained linear regressions and their respective 95% prediction limits. Tables 7 and 8 summarize the linear regression slope, y -intercept terms, r^2 and standard error (S_{yx}) terms for the leeway speed, downwind component of leeway and crosswind components of leeway. Since separation of the crosswind components of leeway resulted in two smaller data sets, they were re-combined by adding the negative of the Negative Crosswind components to the Positive Crosswind Components and performing the regression of the combined data set against the 10-meter wind speed, shown in Fig 25. With this limited data set we were unable to collect sufficient data to characterize differences between the positive and negative components of the crosswind leeway (see Tables 8 and 9).



(A)

(B)

Figure 21. (A) Drift runs of the Skiff. The starting point is at the squares, run number is near the end of the run. (B) Drift runs of skiff and Sunfish. Drift runs of the same color occurred at the same time. See Table 1 for exact start and end time of usable data records.

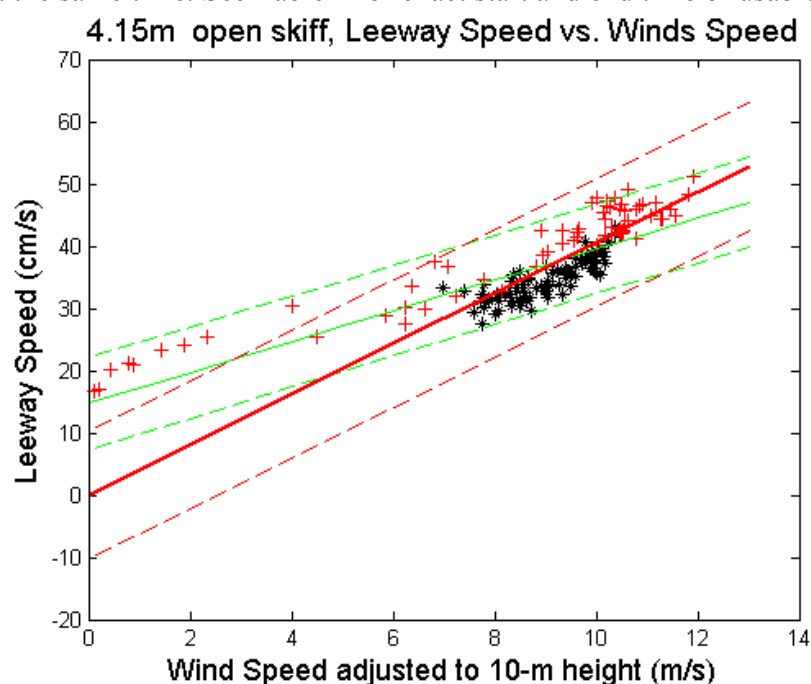


Figure 22. Leeway Speed (cm/s) versus Wind Speed adjusted to 10-m height for the 4.15 m open skiff. Unconstrained linear regression mean (solid) and 95% confidence levels (dash) are plotted in green. Constrained linear regression is plotted in red. Black asterisks (*) represent Run 4 and red pluses (+) represent Run 5.

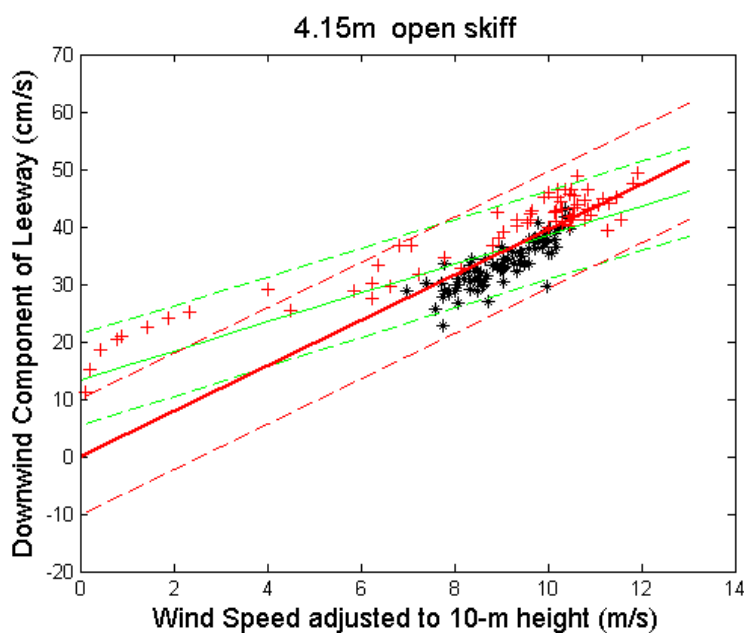


Figure 23. Downwind Component of Leeway (cm/s) versus Wind Speed adjusted to 10-meter height for the 4.15 m open skiff. Unconstrained linear regression mean (solid) and 95% confidence levels (dash) are plotted in green. Constrained linear regression is plotted in red. Black asterisks (*) represent Run 4 and red pluses (+) represent Run 5.

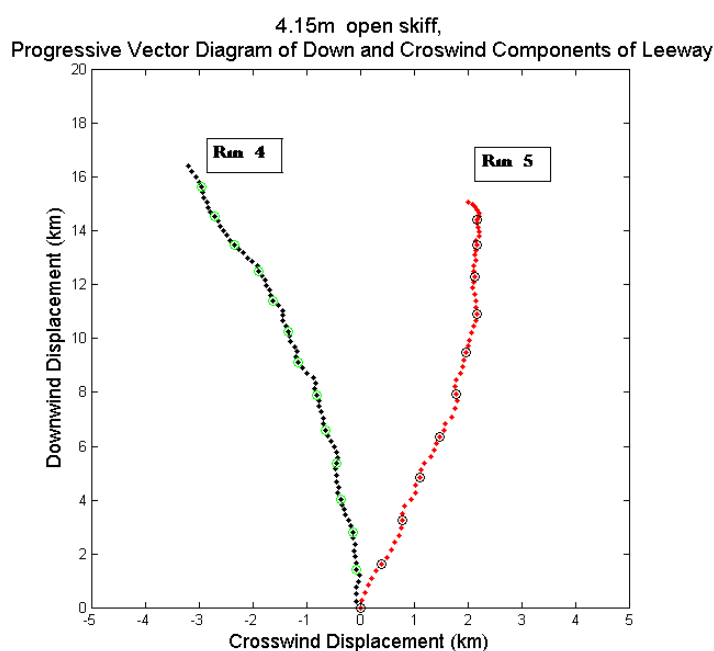


Figure 24. Progressive Vector Diagram (PVD) of the Downwind and Crosswind components of Leeway Displacement for the 4.15m Open Skiff. Downwind is up, and positive Crosswind is to the right. Displacement is in kilometers. Hourly intervals are indicated by a hatched point every 6th point. Crosswind displacement is exaggerated 2x downwind displacement. Black represents Run 4 and red represents Run 5.

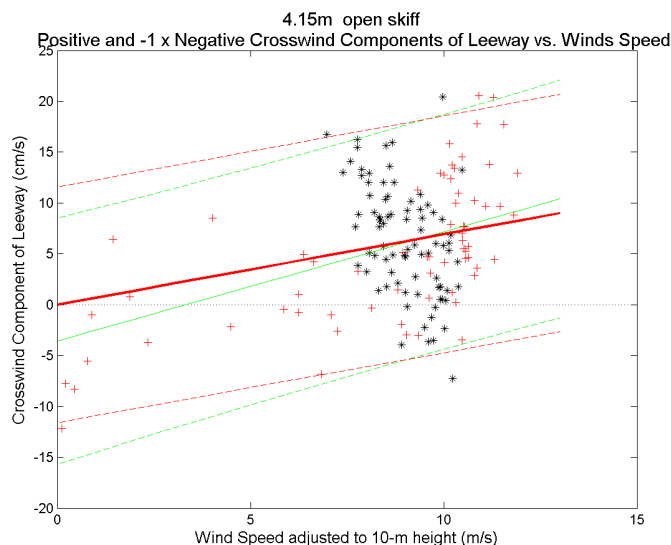


Figure 25. Positive and one minus the negative Crosswind Component of Leeway (cm/s) versus Wind Speed adjusted to 10-meter height for the 4.15m open skiff, from Run 5. Unconstrained linear regression mean (solid) and 95% confidence levels (dash) are plotted in green. Constrained linear regression is plotted in red. Run 5 positive CWL are plotted as red (+). Left-of-downwind (negative) CWL values from Run 4 are plotted as black asterisks (*).

The Leeway of the Sunfish Sailboat

Leeway data was successfully collected from six drift runs for the Sunfish during the September 2009 Fedje and Andfjord Leeway Drift experiments. The drift runs of the Sunfish that successfully returned concurrent leeway and wind data are summarized in Table 5. The Sunfish instrumentation simulated the weight of survivors onboard. A plywood daggerboard was used for each drift run, but broke off, hence the runs include leeway drift data with and without daggerboard.

The leeway speed and downwind component of leeway of the Sunfish versus the wind speed adjusted to the 10-m height are shown in Figs 26 and 27, along with the unconstrained and constrained linear regressions and their respective 95% prediction limits. Tables 8 and 9 summarize the linear regression slope, y -intercept terms, r^2 and standard error (S_{yx}) terms for the leeway speed, downwind component of leeway and crosswind components of leeway. The crosswind components of leeway for the Sunfish were segregated into positive and negative values after inspecting the progressive vector diagram of the downwind and crosswind components of leeway displacement (Fig 28), and the time series of crosswind components of leeway (not shown). In Fig 28, one major shift in crosswind component from negative (left of downwind) to positive crosswind (right of downwind) is indicated by the arrow. As before, the resulting subsets were re-combined by changing the sign of left-drifting crosswind estimates and adding them to the right-drifting (positive) crosswind estimates before performing the regression against the 10-m wind speed (Fig 29 and Tables 8 and 9).

The drifts (GPS positions) of the Sunfish are shown in Fig 30 for each of the six runs. Labels are plotted near the end of each runs.

Table 5. Summary of Sunfish Leeway Drift Runs.

Drift Object Run	Start		End		Duration		10 m Wind Speed Range
	Time	Date	Time	Date	Hr	Min	
	UTC		UTC				m/s
Run 1	21:00	10 Sept. 2009	07:40	11 Sept. 2009	10	40	3.8 □ 6.1
Run 2*	11:00	11 /9/2009	14:30	11 /9/2009	2	30	6.6 □ 9.3
Run 3	20:20	12 /9/2009	11:20	13 /9/2009	15	00	7.0 □ 11.0
Run 4	15:10	13 /9/2009	07:00	14/9/2009	10	40	1.4 - 11.9
Run 5	09:40	24/9/2009	09:10	25/9/2009	23	30	0.1 □ 15.2
Run 6	17:50	25/9/2009	20:00	25/9/2009	2	00	14.9 □ 21.4

* The Sunfish was capsized during recovery after Run 2 and the WeatherPak data was lost, leaving only Sonic wind speed from Skiff Run 2. Without wind direction estimates, the leeway speed was not decomposable into downwind and crosswind components.

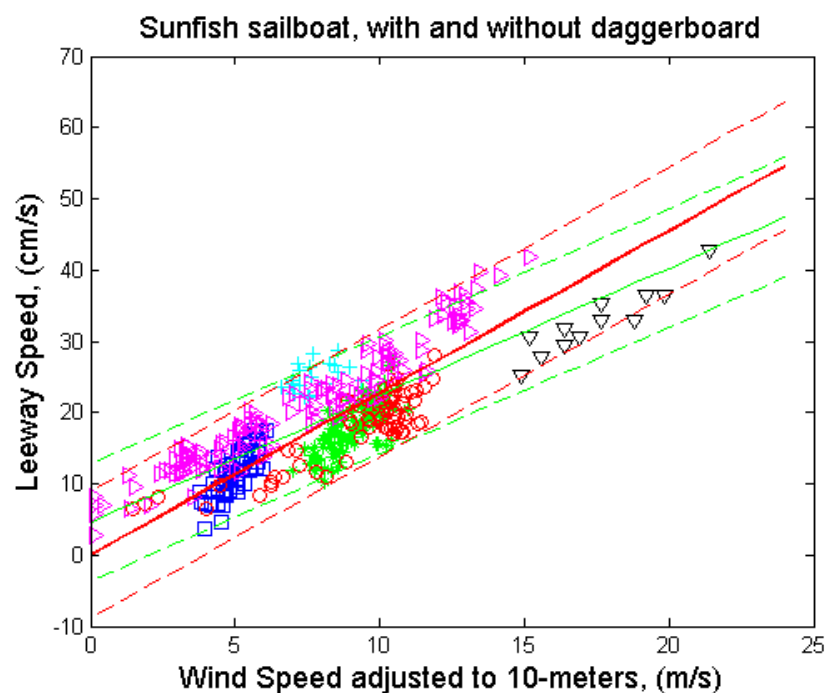


Figure 26. Leeway Speed (cm/s) versus Wind Speed adjusted to 10-meter height for the Sunfish. Unconstrained linear regression mean (solid) and 95% confidence levels (dash) are plotted in green. Constrained linear regression is plotted in red. Run 1 data are plotted in blue (□) and Run 3 in red (○).

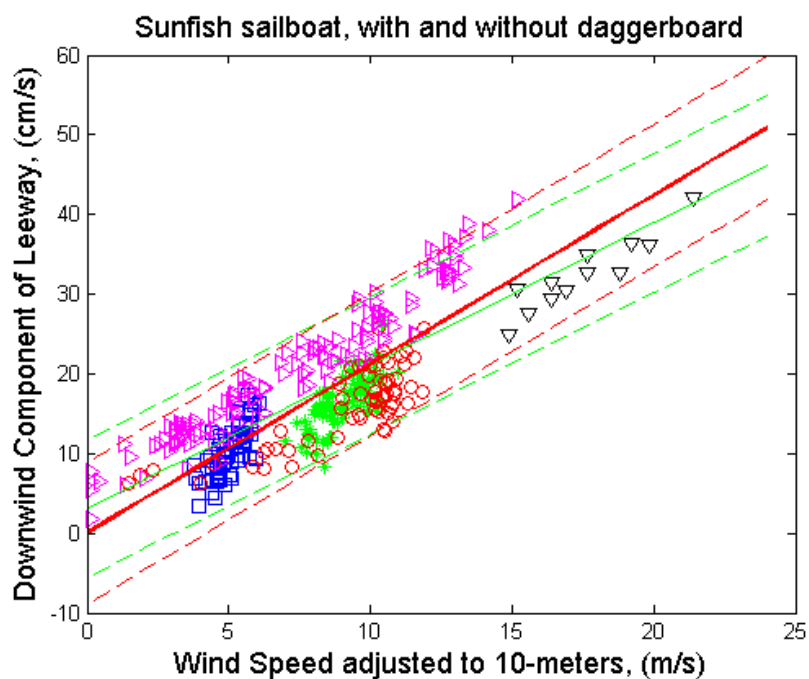


Figure 27. Downwind Component of Leeway (cm/s) versus Wind Speed adjusted to 10-meter height for the Sunfish. Unconstrained linear regression mean (solid) and 95% confidence levels (dash) are plotted in green. Constrained linear regression is plotted in red. Run 1 data are plotted in blue (□) and Run 3 in red (o).

Sunfish,
Progressive Vector Diagram of Down and Crosswind Components of Leeway

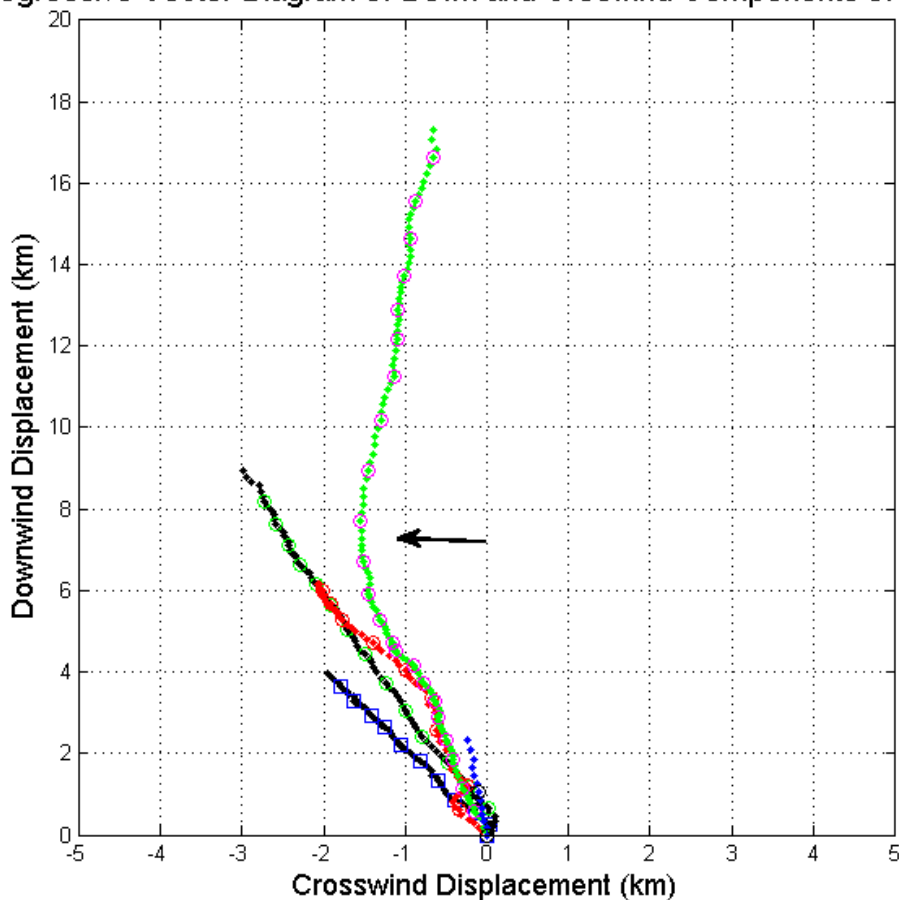


Figure 28. Progressive Vector Diagram (PVD) of the Down and Crosswind components of Leeway Displacement, for the Sunfish. Downwind is up, and positive Crosswind is to the right. Displacement is in kilometers. Hourly intervals are indicated by a circled point every 6th point. Run 1 data are plotted in black with blue squares. Run 3 is black with green circles. Run 4 is marked with red, Run 5 is marked with green, and Run 6 is marked with blue. Horizontal black arrows indicate major shifts in the sign of the crosswind component of leeway during Run 5.

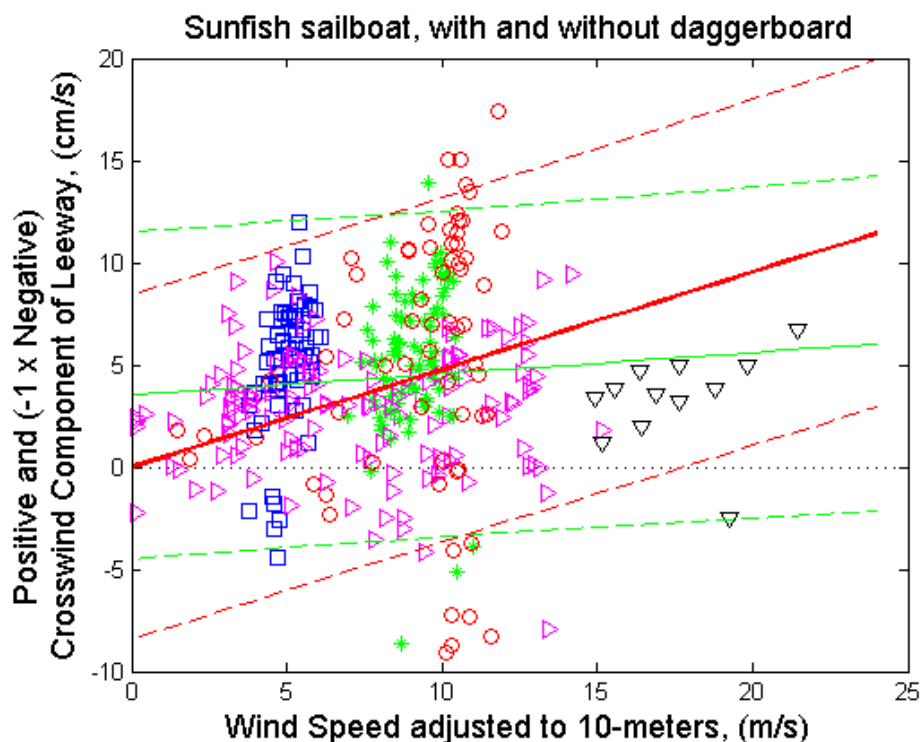


Figure 29. Positive and minus one times the Negative values of the Crosswind Component of Leeway (cm/s) versus Wind Speed adjusted to 10-meter height for the Sunfish. Unconstrained linear regression mean (solid) and 95% confidence levels (dash) are plotted in green. Constrained linear regression is plotted in red. The Positive CWL data are plotted in blue (o) for Run1 and red (o) for Run 3. One minus the Negative CWL data are plotted in blue (+) for Run1 and red (+) for Run 3.

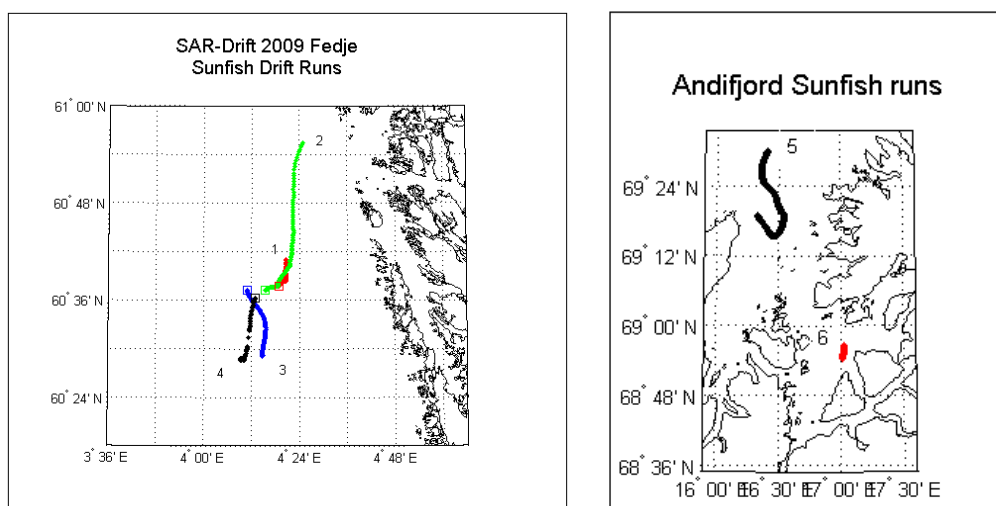


Figure 30. Sunfish drift runs near Fedje (left) and in Andifjord (right). Drift run number is placed near the end of the drift run.

The Leeway of the PIW in the deceased position

Leeway data were successfully collected from two drift runs for the PIW in the deceased position during the September 2009 Andfjord experiment (Table 6). The trajectories of the PIW in the deceased position are shown in Fig 39 (red).

Table 6. Summary of Leeway Drift Runs for the PIW in the deceased position.

Drift Object Run	Start		End		Duration		10 m Wind Speed Range
	Time	Date	Time	Date	Hr	Min	
	UTC		UTC				m/s
Run 1	17:40	24 Sept. 2009	05:30	25 Sept. 2009	11	50	0.1 □ 14.2
Run 3	05:40	27 Sept. 2009	14:40	27 Sept. 2009	9	00	4.3 □ 13.0

The leeway speed and downwind component of leeway of leeway 10-minute data for PIW in the deceased position versus the 10-m wind speed are shown in Figs 31 and 32, along with the unconstrained and constrained linear regressions and their respective 95% prediction limits. Tables 8 and 9 summarize the linear regression slope, y -intercept terms, r^2 and standard error (S_{yx}) terms for the leeway speed, downwind component of leeway and crosswind components of leeway. The crosswind components of leeway for the PIW in the deceased position were segregated into positive and negative values after inspecting the progressive vector diagram of the downwind and crosswind components of leeway displacement (Fig 33), and the time series of crosswind components of leeway (not shown). The two major shifts in crosswind component from negative (left of downwind) to positive crosswind (right of downwind) are indicated by arrows. The crosswind components were then binned into positive (right-drifting) and negative (left-drifting) components for the regressions shown in Fig 34.

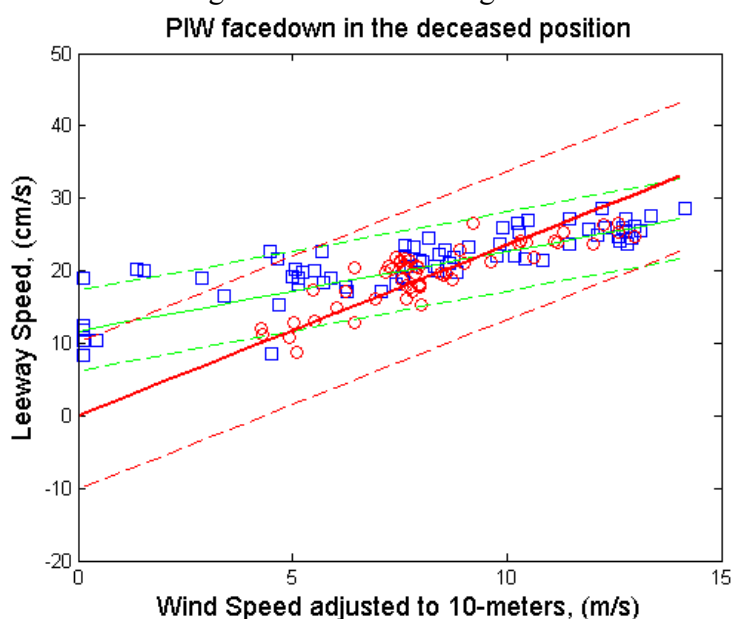


Figure 31. Leeway Speed (cm/s) versus Wind Speed adjusted to 10-m height for the PIW in the deceased position. Unconstrained linear regression mean (solid) and 95% confidence levels (dash) are plotted in green. Constrained linear regression is plotted in red. Run 1 data are plotted in blue (\square) and Run 3 in red (\circ).

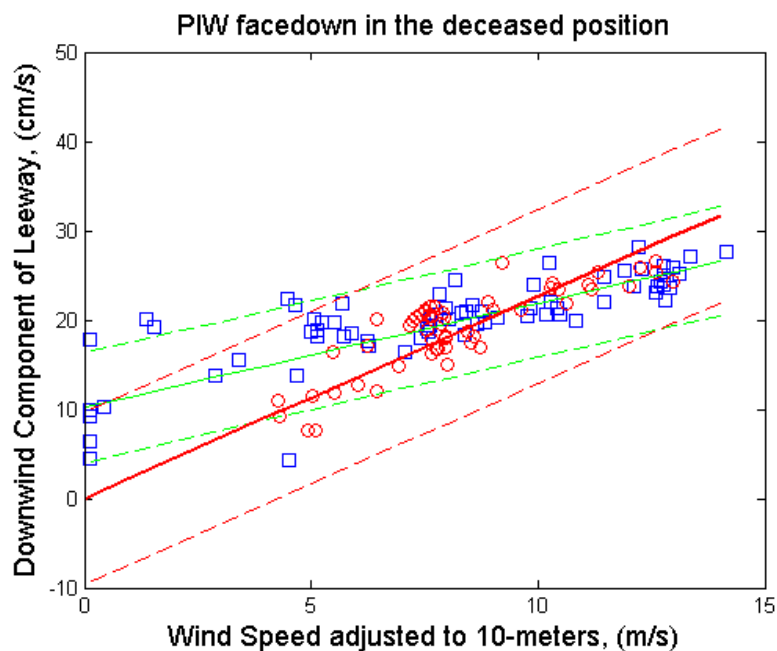


Figure 32. Downwind Component of Leeway (cm/s) versus Wind Speed adjusted to 10-meter height for the PIW in the deceased position. Unconstrained linear regression mean (solid) and 95% confidence levels (dash) are plotted in green. Constrained linear regression is plotted in red. Run 1 data are plotted in blue (\square) and Run 3 in red (\circ).

PIW facedown in the deceased position,
Progressive Vector Diagram of Down and Crosswind Components of Leeway

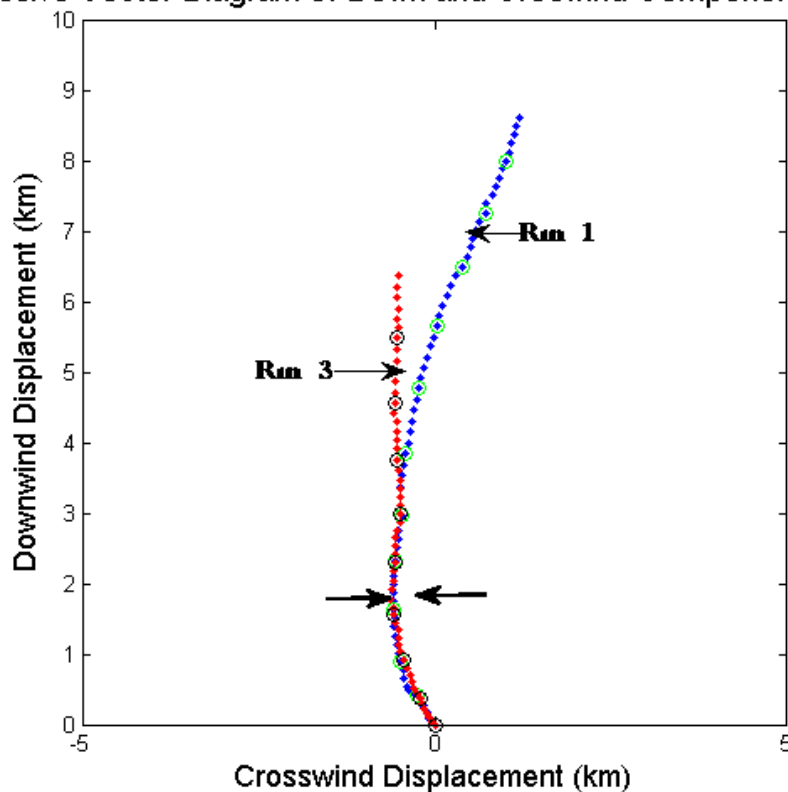


Figure 33. Progressive Vector Diagram (PVD) of the Down and Crosswind components of Leeway Displacement, for the Person-in-the-Water (deceased position). Downwind is up, and positive Crosswind is to the right. Displacement is in kilometers. Hourly intervals are indicated by a circled point every 6th point. Run 1 data are plotted in blue with green circles. Run 3 is red with black circles. Horizontal black arrows indicate major shifts in the sign of the crosswind component of leeway during Runs 1 and 3.

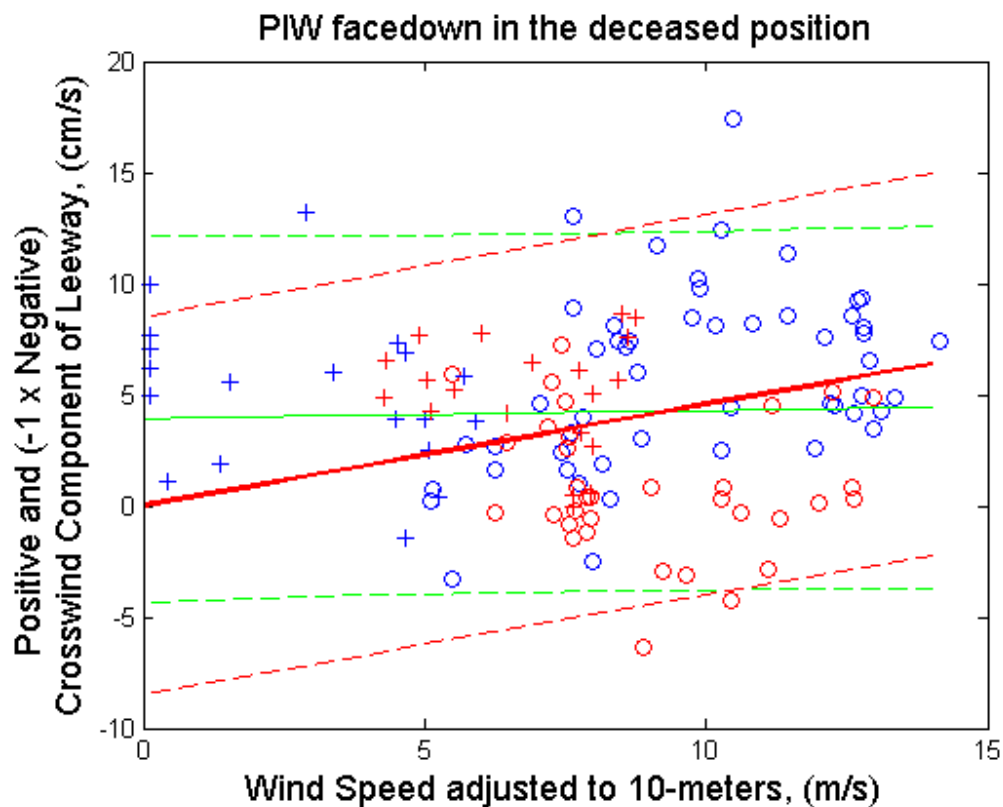


Figure 34. Positive and minus one times the Negative values of the Crosswind Component of Leeway (cm/s) versus Wind Speed adjusted to 10-meter height for the Person-in-the-Water (deceased position). Unconstrained linear regression mean (solid) and 95% confidence levels (dash) are plotted in green. Constrained linear regression is plotted in red. The Positive CWL data are plotted in blue (o) for Run 1 and red (o) for Run 3. One minus the Negative CWL data are plotted in blue (+) for Run 1 and in red (+) for Run 3.

The Leeway of the 20-ft Container

Leeway data were successfully collected from two drift runs for the full-sized 20-foot shipping container during the September 2009 Andfjord Leeway Drift experiment. The drift runs of the 20-foot shipping container that successfully returned concurrent leeway and wind data are summarized in Table 7 (trajectories shown in Fig 39).

Table 7. Summary of Leeway Drift Runs for the 20-ft container

Drift Object Run	Start		End		Duration		10 m Wind Speed Range
	Time	Date	Time	Date	Hr	Min	
	UTC		UTC				m/s
Run 1	09:40	24 Sept. 2009	18:20	25 Sept. 2009	8	40	1.3 □ 10.2
Run 2	05:40	27 Sept. 2009	16:40	27 Sept. 2009	11	00	4.3 □ 14.3

The leeway speed and downwind component of leeway of leeway 10-minute data for Full-sized 20-foot shipping container versus the wind speed adjusted to the 10-meter height are shown in Figs 35 and 36, along with the unconstrained and constrained linear regressions and their respective 95% prediction limits. Tables 8 and 9 summarize the linear regression slope, y -intercept terms, r^2 and standard error (S_{yx}) terms for the leeway speed, downwind component of leeway and crosswind components of leeway. The crosswind components of leeway for the 20-ft container were segregated into positive and negative values after inspecting the progressive vector diagram of the downwind and crosswind components of leeway displacement (Fig 37), and the time series of crosswind components of leeway (not shown). In Fig 37, the major shift in crosswind component from negative (left of downwind) to positive crosswind (right of downwind) is indicated by an arrow. Based upon this and the time series, the crosswind components were binned into either positive or negative components for the regressions shown in Fig 38 the positive and negative components of leeway for the 20-ft container versus the 10-meter wind speed, along with their linear constrained and unconstrained regressions.

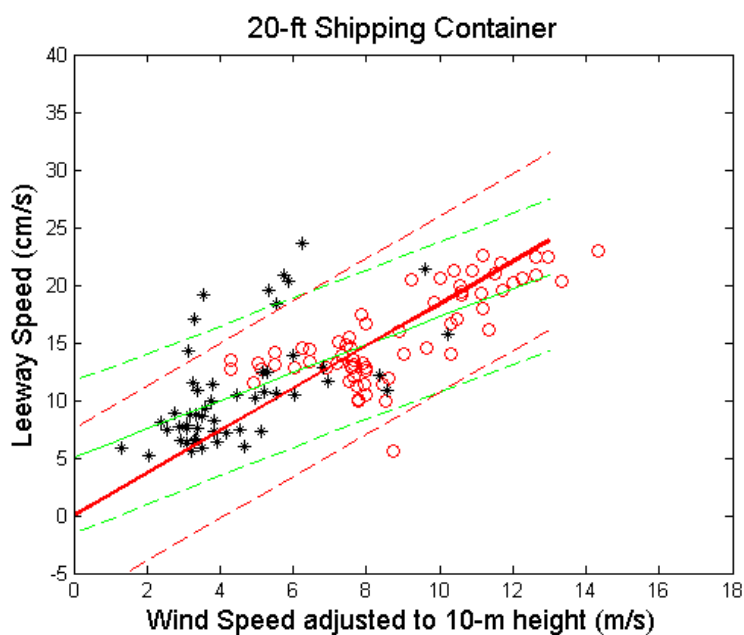


Figure 35. Leeway Speed (cm/s) from the AquaDopp versus Wind Speed from the WeatherPak adjusted to 10-meter height for the Full-sized 20-foot shipping container. Unconstrained linear regression mean (solid) and 95% confidence levels (dash) are plotted in green. Constrained linear regression is plotted in red. Run 1 data are plotted in black (*) and Run 2 in red (o).

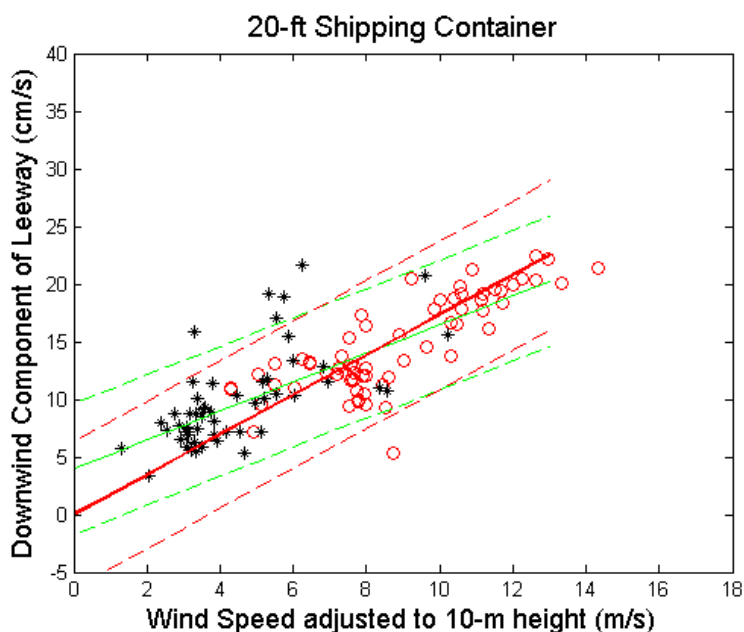


Figure 36. Downwind Component of Leeway (cm/s) versus Wind Speed adjusted to 10-meter height for the Full-sized 20-foot shipping container. Unconstrained linear regression mean (solid) and 95% confidence levels (dash) are plotted in green. Constrained linear regression is plotted in red. Run 1 data are plotted in black (*) and Run 2 in red (o).

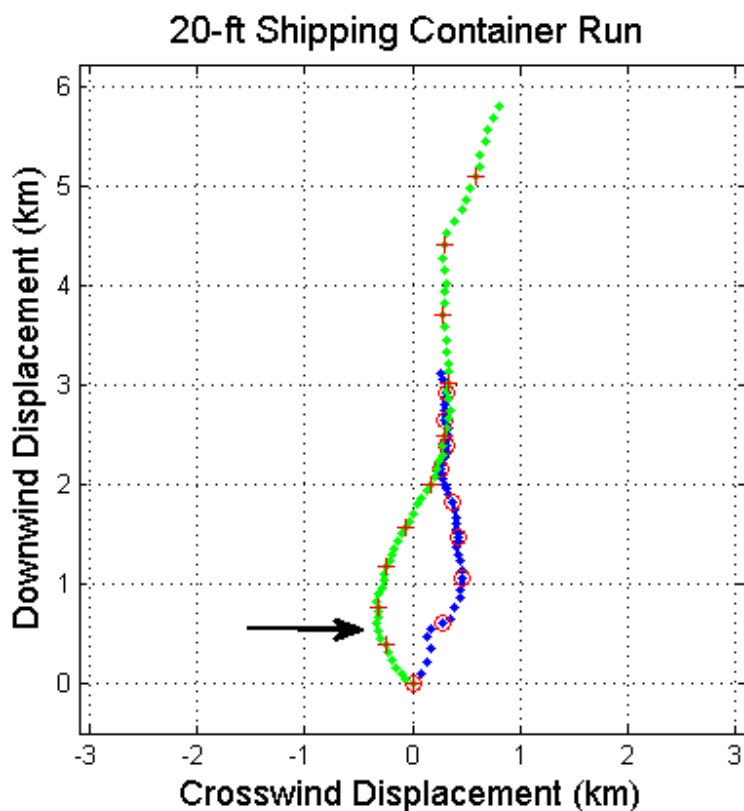


Figure 37. Progressive Vector Diagram (PVD) of the Downwind and Crosswind components of Leeway Displacement, for the 20-ft container. Downwind is up, and positive Crosswind is to the right. Displacement is in kilometers. Hourly intervals are indicated by a circled point every 6th point. Run 1 data are plotted in blue with red circles, and Run 2 in green with red crosses. Horizontal black arrow indicates a major shift in the sign of the crosswind component of leeway after the ninth sample of Run 2.

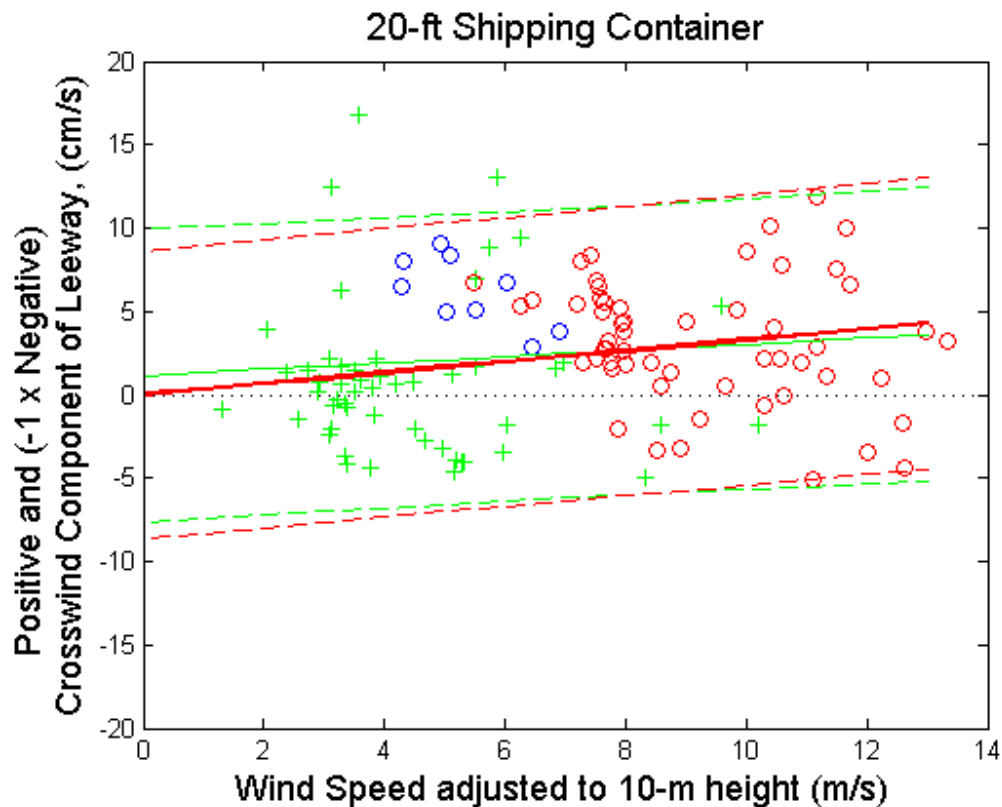


Figure 38. Positive and minus one times the Negative values of the Crosswind Component of Leeway (cm/s) versus Wind Speed adjusted to 10-meter height for the 20-ft container. Unconstrained linear regression mean (solid) and 95% confidence levels (dash) are plotted in green. Constrained linear regression is plotted in red. The Positive CWL data are plotted in green (+) for Run1 and red (o) for Run 2. One minus the Negative CWL data are plotted in blue (o) for first nine samples of Run 2.

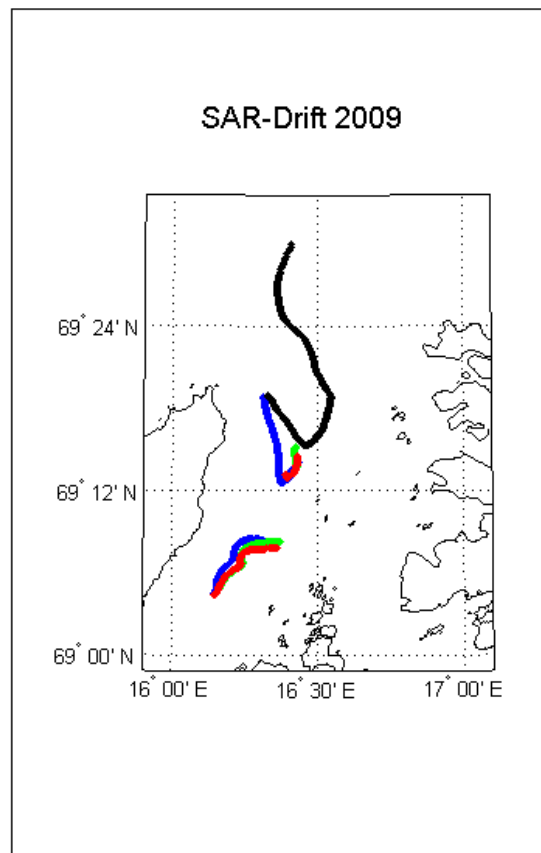


Figure 39. GPS positions from the Andfjord runs. The 20-ft container data are plotted in blue, PIW in the deceased position in red, the AIS buoy in green and the Sunfish in black.

Table 8. Unconstrained Linear Regression Parameters

Drift Object	Leeway Speed				DWL				+CWL			
	Slope (%)	Y (cm/s)	Syx (cm/s)	r ²	Slope (%)	Y (cm/s)	Syx (cm/s)	r ²	Slope (%)	Y (cm/s)	Syx (cm/s)	r ²
L-MK2	0.961	7.27	5.44	0.18	1.07	4.47	6.55	0.16	0.41	1.15	4.13	0.07
Skiff	2.486	14.72	3.63	0.71	2.52	13.37	3.87	0.69	1.07	-3.58	5.82	0.15
Sunfish	1.78	4.62	4.16	0.68	1.79	3.09	4.37	0.67	0.10	3.53	4.05	0.01
PIW deceased	1.10	11.7	2.74	0.63	1.17	10.2	3.04	0.61	0.04	3.9	4.05	0.001
Container	1.22	5.08	3.25	0.57	1.25	3.96	2.81	0.65	0.19	1.14	4.36	0.02

Table 9. Constrained through zero, Linear Regression Parameters

Drift Object	Range of 10m Wind Speed (m/s)	# of 10-minute samples	Leeway Speed			DWL			+CWL		
			Slope (%)	Syx (cm/s)	r ²	Slope (%)	Syx (cm/s)	r ²	Slope (%)	Syx (cm/s)	r ²
L-MK2	0.0 □ 11.9	325	1.78	5.88	0.04	1.57	6.69	0.12	0.54	4.14	0.06
Skiff	0.1 to 11.9	149	4.06	5.18	0.41	3.95	5.12	0.45	0.69	5.87	0.13
Sunfish	0.1 □ 21.4	371/386	2.28	4.52	0.61	2.12	4.53	0.64	0.48	4.28	-0.11
PIW deceased	0.1 to 14.2	125	2.35	5.15	-0.31	2.26	4.87	-0.006	0.46	4.29	-0.13
Container	1.3 □ 14.3	118	1.83	3.83	0.39	1.73	3.22	0.53	0.33	4.36	0.006

Jibing Frequency

Allen (2005) studied the jibing of a drifting object, defined as a prolonged change of tack (sign change) of the crosswind component of leeway (CWL). Jibing is a term commonly used in sailing, where it is understood as the sailboat changing its tack relative to the downwind direction by passing its stern through the wind. Jibing is also observed in the leeway of drifting objects and the frequency of these changes in CWL is an important element for modeling search areas. With no changes in CWL sign, the initial Monte Carlo probability distribution will rapidly separate into two areas of high probability depending on whether the object has a left or right tack. If the object jibes, the probability distribution will over time "fill in" the central area between the two dominant search areas. The more frequent the jibing, the more central the distribution will be.

Jibes or changes in CWL sign can occur abruptly from one ten-minute sample to the next or gradually over several sampling periods. It may be difficult to quantify these events and we have resorted to subjective inspection of the time series and the PVDs to split the records into either negative (left-drifting) or positive (right-drifting) segments.

Allen (2005) was unable to describe either the dynamics of jibing or provide a statistical model of jibing as function of wind speed or the object shape but provided an estimated jibing frequency of 3-7% per hour. We have quantified the jibing frequency per hour from this experiment to range from 1-10%, in rough agreement with Allen (2005). A summary is found in Table 10.

Table 10. Frequency of significant changes between positive and negative crosswind components of leeway.

Drift Object	# of 10-minute samples	Hours:Minutes of Samples	CWL switches (jibes)	Frequency Per hour (%)
WWII mine L-MK2	325	54:10	0	0.0
4.15 m Skiff	149	24:50	0	0.0
Sunfish	371	61:50	1	1.6
PIW deceased	405	20:50	2	9.6
20-ft Container	118	19:40	1	5.1

The Leeway of Containers As a Function of The Immersion Ratio

Daniel *et al.* (2002) estimated the leeway ratio (leeway speed / wind speed) as function of the immersion ratio. It was assumed that the drag coefficients for both air and water were between 0.8 and 1.2 for containers and chose 1.0 for both parameters, see Fig 2 of Daniel *et al.* (2002). The 1:3.3 sized 40-foot shipping container (Breivik *et al.*, 2010) immersed to roughly 70% exhibited a leeway rate of 2.0% \pm 0.3% of the 10-m wind speed. The full-sized 20-foot shipping container studied here was immersed to roughly 80%. Its leeway rate (see Table 9) was 1.83% \pm 0.38% of the 10-m wind speed. Fig 40 shows estimates of the two containers (red cross for the scaled-down 40-ft container and blue cross for the full-size 20-ft container) along with curves of drift speed as a function of immersion ratio (%), following Eq (2) of Daniel *et al.* (2002) with air drag coefficients between 0.7 and 1.15. Our two containers appear to have a leeway to wind ratio which roughly follows the formula assumed by Daniel *et al.* (2002), but the error estimates are rather wide.

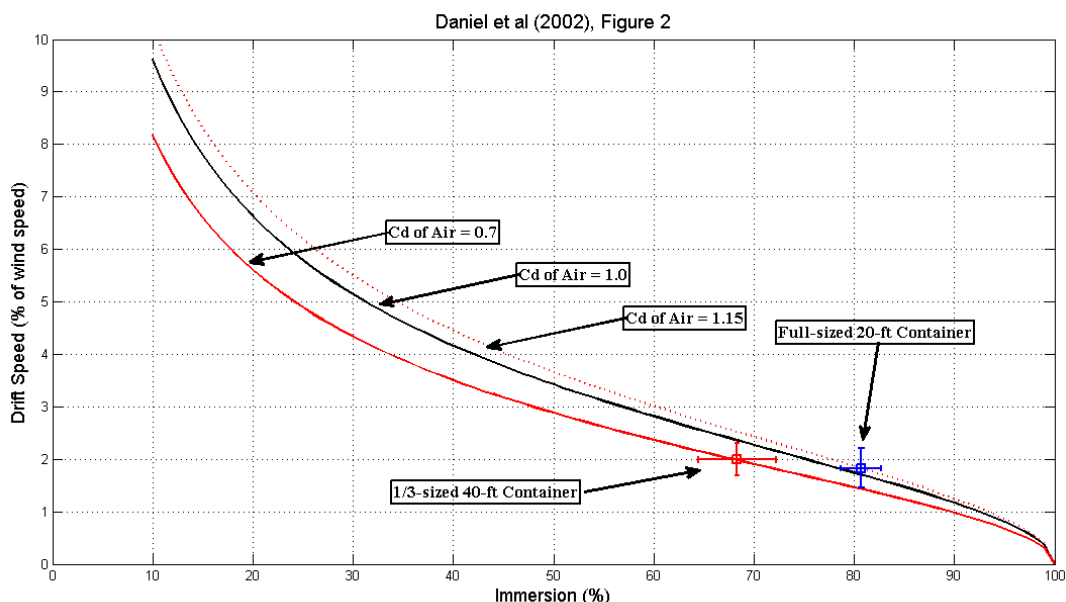


Figure 40. Immersion ratio (%) of containers versus leeway ratio (% of 10-m wind speed). Daniel *et al.* (2002) assumed $C_D = 1.0$. (black line). Here we contrast that with $C_D = 0.7$ (red solid line) and 1.15 (red dashed line). to compare the leeway rates and their for the scaled-down (1:3.3 sized) 40-ft container (red cross) and the full sized 20-ft container (blue cross). Leeway ratio and their uncertainty are plotted as crosses.

Summary and Recommendations

Leeway data were successfully collected on five drifting objects; a WWII Mk2 mine, a 4.15 m open skiff, a Sunfish, a Person-in -Water in the deceased position, and a full sized 20-foot shipping container immersed at 80%. In addition, the displacement of a drifting buoy (denoted MOB) was studied, but no leeway estimates were attempted.

A total of 54 hours of data has now been collected on the WWII Mk2 mine and 64 hours of data has been collected on the Sunfish sailboat. This is sufficient to estimate the basic leeway coefficients for both downwind and crosswind leeway components.

The skiff commonly used along the Norwegian coast should continue to be a high priority for study as the amount of data collected to date is limited. A skiff in the capsized configuration should also be studied, as there are no leeway estimates on capsized small, open boats.

All PIW categories are important and this study demonstrates that light instrumentation now exists that can be attached to PIW manikin. The next step is to fully integrate the instrumentation into a manikin with realistic hydrodynamic characteristics and study PIWs in all their typical distress configurations, type I and II personal flotation devices (PFD) or life vests, PIW in a type III PFD, PIW in survival suit, and deceased.

We have demonstrated successful deployment and recovery of a full-sized 20-foot shipping container, but more immersion levels must be studied before the full leeway range of containers has been explored.

Studies of the jibing frequency should be continued and in time different object categories should be assigned specific jibing frequencies, but for the time being the datasets are too short to allow such differentiation.

It is recommended that the five drift objects here studied be added to SAR planning tools using the coefficients from either Table 8 or 9.

Acknowledgment

The authors would like to direct their sincere thanks to the Norwegian Coast Guard and the competent crews of CGV Aalesund and CGV Harstad, without whom these drift experiments could not have been carried out. We further acknowledge the support from the French-Norwegian Foundation and Eureka through the SAR-Drift project (E!3652).

References

Allen, A.A. and J.V. Plourde, 1999. *Review of Leeway; Field Experiments and Implementation*, USCG R&D Center Report CG-D-08-99

Allen, A.A., 2005. *Leeway Divergence*, USCG R&D Center Report CG-D-05-05

Breivik, Ø and A A Allen, 2008. An operational search and rescue model for the Norwegian Sea and the North Sea, *J Mar Syst*, **69**(1-2), pp 99-113, DOI:10.1016/j.jmarsys.2007.02.010

Breivik, Ø, A Allen, C Maisondieu and J C Roth, 2010. The Leeway Field Method, *Submitted to Applied Ocean Research*

Daniel, P., J.Gwénaële, F.Cabio, h, Y Landau, and E Loiseau, 2002. Drift Modeling of Cargo Containers, *Spill Science and Technology Bulletin*, **7**(5-6), pp 279-288.

Davidson, F J M, A Allen, G B Brassington, B , P Daniel, M Kamachi, S Sato, B King, F Lefevre, M Sutton, H Kaneko, 2009. Applications of GODAE ocean current forecasts to search and rescue and ship routing, *Oceanography*, **22**(3), pp 176-181

Hackett, B, Ø Breivik and C Wettre, 2006. Forecasting the drift of objects and substances in the oceans in *Ocean Weather Forecasting: An Integrated View of Oceanography*, E P Chassignet, J Verron (ed), Springer, pp 507-524

Neter, J., M.H. Kutner, C.J. Nachtsheim, and W. Wasserman, 1996. *Applied Linear Statistical Models*, Fourth Edition, Irwin, Inc. Chicago, IL

Smith, S.D., 1988. Coefficients for Sea Surface Wind Stress, Heat Flux, and Wind Profiles as a Function of Wind Speed and Temperature, *J. Geophys Res.* **93**(C12), pp. 15,467-15,472